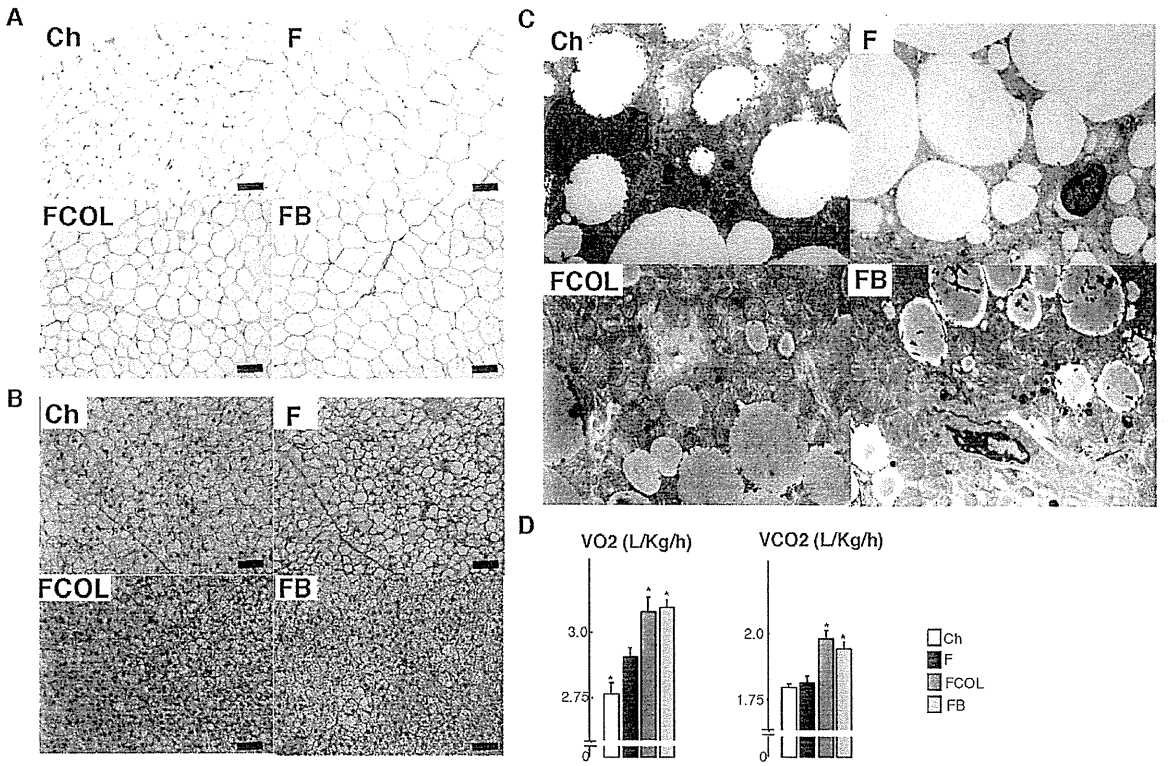

Figure 2. BABR increase energy expenditure. Hematoxylin and eosin (HE) stained epWAT (A) and BAT (B) sections of C57BL/6J animals treated with control or HF diet when indicated combined with colestimide or CA as specified in Fig. 1. Scale bar, 50 μm. (C) BAT analysis by transmission electron microscopy. (D) Averaged O_2 consumption (VO_2) and CO_2 production (VCO_2) as measured by indirect calorimetry in mice on the different diets as indicated. Data are expressed as the mean +/− SEM (n = 5–6). * ($P<0.05$) or ** ($P<0.01$) versus F.
doi:10.1371/journal.pone.0038286.g002

increased the relative contribution of CA and its derivatives, most notably tauroCA. Bile acids derived from chenodeoxyCA such as tauromuriCA were decreased by both BA supplementation and BABR treatment (Fig. 4 and [22]). BABR preferentially sequesters mono- and di-hydroxy BA and prevent them from enterohepatic recirculation hence inducing the de novo synthesis of CA.

Discussion

In the present study, we show that administration of BABR stimulated energy expenditure mediated by BAT, thereby preventing and reversing diet-induced obesity in mice. This phenomenon was accompanied by an improved glucose tolerance and insulin sensitization in a diet-induced obesity model (C57BL6/J (Fig. 1)). BABR also improved glucose tolerance in KK-A^y mice (Text S1 and Fig. S1). Brown adipose tissue is recently recognized as an important tissue of thermogenesis and energy homeostasis not only in rodents but also in man [31–33]. Our results indicate that therapy with colestimide, a new and better formulated BABR when compared with cholestyramine, could improve metabolic control also in humans suffering from the metabolic syndrome. In fact, colestimide decreased fasting glucose levels, but also reduced body weight, BMI, and visceral fat mass [34]. Furthermore, BABR was reported to improve obesity, insulin sensitivity and glycemic control in diabetes mellitus mouse model [25]. Furthermore, there is clinical evidence suggesting that BABR such as colesevelam may improve both lipid control and glycemic control in patients with type 2 diabetes that receive oral antihyperglycemic medications [35–37] [38,39]. Combined with the limited systemic toxicity ofBABR, which isnot absorbed, these compounds could constitute a significant advance in our therapeutic armamentarium to combat against metabolic syndrome. Although there is some evidence that the beneficial effects of BABR may be mediated through FXR, LXR, FGF15/19, and TGR5, but the exact molecular mechanisms are not yet clearly defined.

On a molecular and cellular level, BABR improves metabolic homeostasis through effects on liver and BAT (Fig. 5). The effects on liver are well known and include an induction of cholesterol and BA biosynthesis, subsequent to the fecal loss of bile acids caused by the BABR treatment. This underlies the cholesterol-lowering effect of BABR. The metabolic effects on BAT have not been reported before and phenocopy the changes seen after treatment of rodents with primary BA, such as CA [22]. This is surprising, since treatment with BABR and BA has opposite actions on most parameters of BA homeostasis. CA administration increases FXR activation, whereas BABR treatment decreases it. CA administration decreases the BA synthesis, whereas BABR treatment increases it. However, BABR and CA had similar effects on BA composition. Both treatments increased the relative contribution of CA and its derivatives, most notably deoxyCA, tauro-deoxyCA and tauroCA. Bile acids derived from chenodeox-

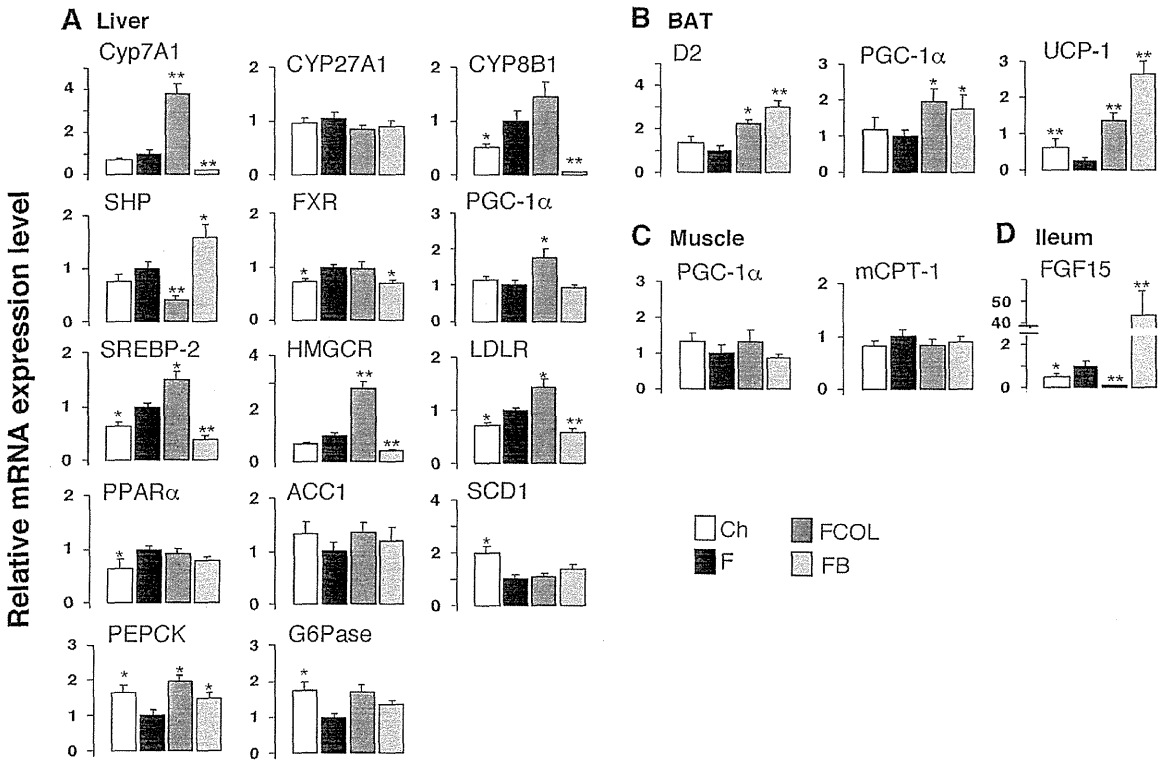

Figure 3. Gene expression in liver, BAT, muscle and ileum. (A) mRNA expression levels of *Cyp7a1*, *Cyp8b1*, *Cyp27a1*, *Shp*, *Fxr*, *Pgc-1α*, *Pepck*, *G6Pase*, *Srebp-2*, HMG-CoA reductase, LDL-Receptor, *Pparα*, *Acc1* and *Scd1* were determined using quantitative RT-PCR in liver of C57BL/6J mice treated as described in Fig. 1A. (B) mRNA expression levels of *D2*, *Pgc-1α* and *Ucp-1* in BAT. (C) *Pgc-1α* and *mCpt-1* in muscle. (D) *Fgf15* in ileum. Treatments and abbreviations are identical to those specified in Fig. 1A. Mice were fasted 4 hours before sacrifice and tissue collection. Data are expressed as the mean +/− SEM (n = 5–6). * ($P<0.05$) or ** ($P<0.01$) versus F.
doi:10.1371/journal.pone.0038286.g003

yCA such as muriCA and tauromuriCA were decreased. In addition to our studies in mice, colestimide treatment of hypercholesterolemia patients significantly increased CA in bile [40]. The most likely explanation for this specific increase in BA species derived from CA, is the fact that colestimide has a high adsorptive capacity for mono- and di-hydroxy BA like chenodeoxyCA and lithoCA, but a relative low capacity for the tri-hydroxy BA such as CA. In addition, the induced BA biosynthesis during colestimide treatment might produce more CA than chenodeoxyCA [41]. Increased BA pool size and plasma BA levels are fine indicator for TGR5 activation [22] [17]. This time, we focus on the importance of bile acid composition to improve metabolic status. TGR5 is activated by almost all BA including mono- and di-hydroxy BA. Some of the BA like ursodeoxyCA have little activity on TGR5, but no inhibitory BA was identified in our test of over 60 BA and BA derivatives for antagonistic effects on TGR5 (data not shown). Most importantly, BABR administration induced levels of tauroCA, a relatively potent TGR5 agonist [22], which could be the key to the anti-metabolic syndrome effect of BABR administration. In agreement with this, reduction of BA pool size and tauroCA levels by the administration of the synthetic FXR agonist GW4064, exacerbated the effects of HF feeding [17].

It is conceivable that BABR, such as colestimide and cholestyramine that are mainly active in the intestinal tract, could affect the production of incretins, such as FGF15, cholecystokinin (CCK) and glucagon like peptide-1 (GLP-1). FGF15 is interesting in this respect, since transgenic mice that overexpress the human *Fgf15* ortholog *Fgf19* in the muscle or in a more general pattern have increased metabolic rate and decreased adiposity [42]. BABR, however, decreases expression of *Fgf15* (Fig. 3D), whereas CA has the opposite effect, making it unlikely that it underlies the common metabolic effects of BABR. GLP-1 has glucose-dependent insulinotropic actions on the pancreatic beta-cells and has recently been associated with bile acids because its release was stimulated in an enteroendocrine cell line via TGR5, a GPCR specific for bile acids [23]. BABR may have an effect on the intestinal secretion of GLP-1, according to recent reports [43]. Indeed, we found that GLP-1 secretion was stimulated by BABR administration (unpublished data), which may contribute to the other beneficial effects of BABR. CCK is another good candidate, since cholestyramine can increase CCK production but also pancreatic beta cell function [44–45]. In addition CCK has been linked to increased sympathetic activity to BAT [46–47]. To date, effects of BABR on incretins and BAT have not been sufficiently studied.

Taken together, our data show that BABR activates energy expenditure, resulting in weight loss and improved glucose tolerance in animal models suffering from the metabolic syndrome, in a mechanism very similar to BA administration [22]. The alteration of BA composition, which occurs after BABR

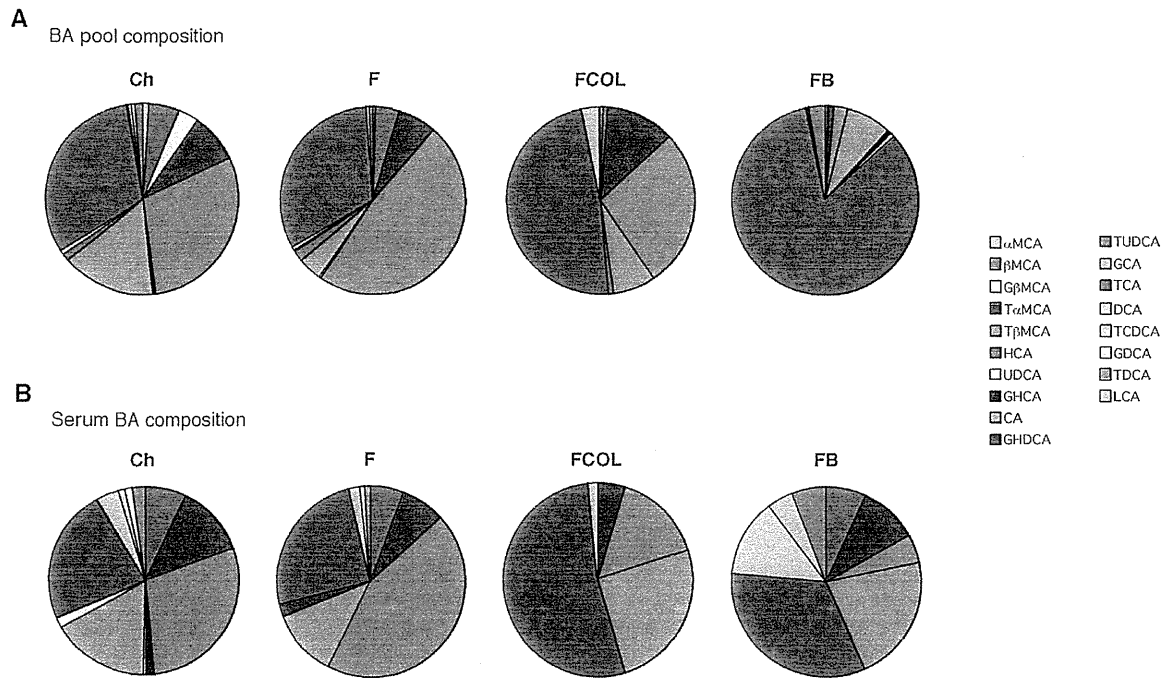

Figure 4. Bile acid composition in the enterohepatic organs and serum. Bile acid composition in the enterohepatic organs and serum of C57BL/6J fed with high fat diet (Fig. 1A) after treatment with colestimide or CA. Undefined abbreviations are: G, glycol; T, tauro; CD, chenodeoxy; D, deoxy; H, hyo; HD, hyodeoxy; UD, ursodeoxy; L, litho; M, muri.
doi:10.1371/journal.pone.0038286.g004

and CA administration, more specifically the increase of tauroCA, may be the key to improve the metabolic status. A recent study in man employing colesevalam treatment in type 2 diabetic patients revealed no correlation energy expenditure with plasma BA levels [48]. Another report showed that BA kinetics caused by BABR administration could not affect the improvement of glycemic control in patients with T2DM [49]. In fact, biophysiological roles and significances of the each composition of the BA profiles might not be identical in human and mice, and it is difficult to make a plain comparison between the report and our result. Futhermore, in the report, the 'BA kinetics' was just a cholic acid or total bile acid synthesis. More precise analysis according to BA profiles, as we performed in this article, would provide a clue to solve the mechanism of improved glycemic control by BABR. These reports illustrate that the mechanisms involved in the beneficial effects of BABR in humans are still controversial and further investigation is warranted. Our previous study demonstrated one of the various mechanisms of BABR in anti-metabolic syndrome effect. Our

Table 2. BA pool size and serum BA concentration in C57BL/6J mice.

	BA pool size (nmol/g Liver+Intestine)	Serum BA (μM)
Ch	9852.6+/−191.2[A]	15.23+/−2.23
F	9130.4+/−261.6	13.83+/−1.80
FCOL	8643.4+/−254.8	11.84+/−1.68
FB	22867.0+/−145.3[B]	18.21+/−1.16[A]

Ch denotes chow, F denotes HF diet, FCOL denotes HF diet+2% w/w colestimide and FB denotes HF diet+0.5% w/w CA as specified in Fig. 1A. Data are expressed as mean +/− SEM (n = 5–6).
[A]$P<0.05$ versus F.
[B]$P<0.01$ versus F.
doi:10.1371/journal.pone.0038286.t002

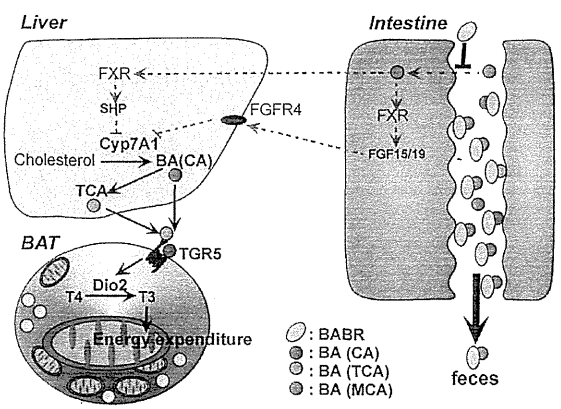

Figure 5. Changes in energy metabolism by BABR administration. Administration of BABR to animals leads to induction of bile acid synthesis and as a consequence a relative increase in CA and TCA. This translates into induced energy expenditure in brown adipose tissue, hence improving obesity and diabetes.
doi:10.1371/journal.pone.0038286.g005

findings in mice could be useful clues to elucidate the signaling functions of BA in man.

Supporting Information

Figure S1 BABR improves metabolic control in KK-A^y mice. (A) Body weight (BW) and food intake change of KK-A^y mice. Ch denotes chow, COL denotes chow+colestimide and CHO denotes chow+cholestyramine. (B) A comparison of the weight of liver, epididymal WAT (epWAT) and BAT fat pads after the different interventions. (C) Serum levels of triglycerides (TG), free fatty acids (FFA), total cholesterol (T-C) in KK-A^y mice on the indicated treatments. (D) Serum levels of glucose and insulin in KK-A^y mice on the indicated treatments. The HOMA-IR is calculated as described in the materials and methods. (E) Glucose levels during an OGTT and IPITT, and area under the curve (AUC) and integrated areas under the curve (iAUC) in KK-A^y mice in the different treatment groups. The OGTT were performed after an overnight fast after 2 weeks of administration. Glucose was administered by gavage at a dose of 1 g/kg. The IPITT were performed after 4 hours fast after 3 weeks of administration. Insulin was injected at a dose of 0.75 U/kg. Data are expressed as the mean +/− SEM (n = 5–6). # ($P<0.05$) or ## ($P<0.01$) versus Ch. Further description about the materials and methods of the experiments is included in "Materials and Methods S1".
(DOC)

Text S1
(DOCX)

Materials and Methods S1
(DOC)

Acknowledgments

The authors thank Pierre Chambon, Ron Evans, Kazuo Suzuki, Kanami Sugimoto-Kawabata, Kaoru Sakai and Satoshi Iwasaki for helpful discussions, and Tomomi Taniguchi, Nadia Messaddeq, Henk Overmars and Marie-France Champy for technical assistance. In memory of Shinya Inoue, who made a great contribution to this study during his short life.

Author Contributions

Conceived and designed the experiments: MW SMH JA. Performed the experiments: MW KM CM T. Sugizaki EA HS YH NKI K. Murahashi. Analyzed the data: MW K. Morimoto. Contributed reagents/materials/analysis tools: T. Sugizaki YH T. Suzuki KS. Wrote the paper: MW K. Morimoto SMH HI JA.

References

1. Makishima M, Okamoto AY, Repa JJ, Tu H, Learned RM, et al. (1999) Identification of a nuclear receptor for bile acids. Science 284: 1362–1365.
2. Parks DJ, Blanchard SG, Bledsoe RK, Chandra G, Consler TG, et al. (1999) Bile acids: natural ligands for an orphan nuclear receptor. Science 284: 1365–1368.
3. Wang H, Chen J, Hollister K, Sowers LC, Forman BM (1999) Endogenous bile acids are ligands for the nuclear receptor FXR/BAR. Mol Cell 3: 543–553.
4. Houten SM, Auwerx J (2004) The enterohepatic nuclear receptors are major regulators of the enterohepatic circulation of bile salts. Ann Med 36: 482–491.
5. Russell DW (2003) The enzymes, regulation, and genetics of bile acid synthesis. Annu Rev Biochem 72: 137–174.
6. Brendel C, Schoonjans K, Botrugno OA, Treuter E, Auwerx J (2002) The small heterodimer partner interacts with the liver X receptor alpha and represses its transcriptional activity. Mol Endocrinol 16: 2065–2076.
7. Goodwin B, Jones SA, Price RR, Watson MA, McKee DD, et al. (2000) A regulatory cascade of the nuclear receptors FXR, SHP-1, and LRH-1 represses bile acid biosynthesis. Mol Cell 6: 517–526.
8. Kerr TA, Saeki S, Schneider M, Schaefer K, Berdy S, et al. (2002) Loss of nuclear receptor SHP impairs but does not eliminate negative feedback regulation of bile acid synthesis. Dev Cell 2: 713–720.
9. Lu TT, Makishima M, Repa JJ, Schoonjans K, Kerr TA, et al. (2000) Molecular basis for feedback regulation of bile acid synthesis by nuclear receptors. Mol Cell 6: 507–515.
10. Sinal CJ, Tohkin M, Miyata M, Ward JM, Lambert G, et al. (2000) Targeted disruption of the nuclear receptor FXR/BAR impairs bile acid and lipid homeostasis. Cell 102: 731–744.
11. Wang L, Lee YK, Bundman D, Han Y, Thevananther S, et al. (2002) Redundant pathways for negative feedback regulation of bile acid production. Dev Cell 2: 721–731.
12. Holt JA, Luo G, Billin AN, Bisi J, McNeill YY, et al. (2003) Definition of a novel growth factor-dependent signal cascade for the suppression of bile acid biosynthesis. Genes Dev 17: 1581–1591.
13. Inagaki T, Choi M, Moschetta A, Peng L, Cummins CL, et al. (2005) Fibroblast growth factor 15 functions as an enterohepatic signal to regulate bile acid homeostasis. Cell Metab 2: 217–225.
14. Stroeve JH, Brufau G, Stellaard F, Gonzalez FJ, Staels B, et al. (2010) Intestinal FXR-mediated FGF15 production contributes to diurnal control of hepatic bile acid synthesis in mice. Lab Invest 90: 1457–1467.
15. Watanabe M, Houten SM, Wang L, Moschetta A, Mangelsdorf DJ, et al. (2004) Bile acids lower triglyceride levels via a pathway involving FXR, SHP, and SREBP-1c. J Clin Invest 113: 1408–1418.
16. Prawitt J, Abdelkarim M, Stroeve JH, Popescu I, Duez H, et al. (2011) Farnesoid x receptor deficiency improves glucose homeostasis in mouse models of obesity. Diabetes 60: 1861–1871.
17. Watanabe M, Horai Y, Houten SM, Morimoto K, Sugizaki T, et al. (2011) Lowering bile acid pool size with a synthetic FXR agonist induces obesity and diabetes through reduced energy expenditure. J Biol Chem.
18. Kawamata Y, Fujii R, Hosoya M, Harada M, Yoshida H, et al. (2003) A G protein-coupled receptor responsive to bile acids. J Biol Chem 278: 9435–9440.
19. Maruyama T, Miyamoto Y, Nakamura T, Tamai Y, Okada H, et al. (2002) Identification of membrane-type receptor for bile acids (M-BAR). Biochem Biophys Res Commun 298: 714–719.
20. Bianco AC, Salvatore D, Gereben B, Berry MJ, Larsen PR (2002) Biochemistry, cellular and molecular biology, and physiological roles of the iodothyronine selenodeiodinases. Endocr Rev 23: 38–89.
21. Puigserver P, Spiegelman BM (2003) Peroxisome proliferator-activated receptor-gamma coactivator 1 alpha (PGC-1 alpha): transcriptional coactivator and metabolic regulator. Endocr Rev 24: 78–90.
22. Watanabe M, Houten SM, Mataki C, Christoffolete MA, Kim BW, et al. (2006) Bile acids induce energy expenditure by promoting intracellular thyroid hormone activation. Nature 439: 484–489.
23. Thomas C, Gioiello A, Noriega L, Strehle A, Oury J, et al. (2009) TGR5-mediated bile acid sensing controls glucose homeostasis. Cell Metab 10: 167–177.
24. Houten SM, Watanabe M, Auwerx J (2006) Endocrine functions of bile acids. Embo J 25: 1419–1425.
25. Kobayashi M, Ikegami H, Fujisawa T, Nojima K, Kawabata Y, et al. (2007) Prevention and treatment of obesity, insulin resistance, and diabetes by bile acid-binding resin. Diabetes 56: 239–247.
26. Homma Y, Kobayashi T, Yamaguchi H, Ozawa H, Sakane H, et al. (1997) Specific reduction of plasma large, light low-density lipoprotein by a bile acid sequestering resin, cholebine (MCI-196) in type II hyperlipoproteinemia. Atherosclerosis 129: 241–248.
27. Picard F, Gehin M, Annicotte J, Rocchi S, Champy MF, et al. (2002) SRC-1 and TIF2 control energy balance between white and brown adipose tissues. Cell 111: 931–941.
28. Mataki C, Magnier BC, Houten SM, Annicotte JS, Argmann C, et al. (2007) Compromised intestinal lipid absorption in mice with a liver-specific deficiency of liver receptor homolog 1. Mol Cell Biol 27: 8330–8339.
29. Sakakura H, Suzuki M, Kimura N, Takeda H, Nagata S, et al. (1993) Simultaneous determination of bile acids in rat bile and serum by high-performance liquid chromatography. J Chromatogr 621: 123–131.
30. Folch J, Lees M, Sloane-Stanley GH (1957) A simple method for the isolation and purification of total lipids from animal tissues. J Biol Chem 226: 497–509.
31. van Marken Lichtenbelt WD, Vanhommerig JW, Smulders NM, Drossaerts JM, Kemerink GJ, et al. (2009) Cold-activated brown adipose tissue in healthy men. N Engl J Med 360: 1500–1508.
32. Cypess AM, Lehman S, Williams G, Tal I, Rodman D, et al. (2009) Identification and importance of brown adipose tissue in adult humans. N Engl J Med 360: 1509–1517.
33. Virtanen KA, Lidell ME, Orava J, Heglind M, Westergren R, et al. (2009) Functional brown adipose tissue in healthy adults. N Engl J Med 360: 1518–1525.
34. Suzuki T, Oba K, Igari Y, Watanabe K, Matsumura N, et al. (2012) Effects of bile-acid-binding resin (colestimide) on blood glucose and visceral fat in Japanese patients with type 2 diabetes mellitus and hypercholesterolemia: an open-label, randomized, case-control, crossover study. J Diabetes Complications 26: 34–39.

35. Garg A, Grundy SM (1994) Cholestyramine therapy for dyslipidemia in non-insulin-dependent diabetes mellitus. A short-term, double-blind, crossover trial. Ann Intern Med 121: 416–422.
36. Bays HE, Goldberg RB, Truitt KE, Jones MR (2008) Colesevelam hydrochloride therapy in patients with type 2 diabetes mellitus treated with metformin: glucose and lipid effects. Arch Intern Med 168: 1975–1983.
37. Fonseca VA, Rosenstock J, Wang AC, Truitt KE, Jones MR (2008) Colesevelam HCl improves glycemic control and reduces LDL cholesterol in patients with inadequately controlled type 2 diabetes on sulfonylurea-based therapy. Diabetes Care 31: 1479–1484.
38. Goldberg RB, Fonseca VA, Truitt KE, Jones MR (2008) Efficacy and safety of colesevelam in patients with type 2 diabetes mellitus and inadequate glycemic control receiving insulin-based therapy. Arch Intern Med 168: 1531–1540.
39. Zieve FJ, Kalin MF, Schwartz SL, Jones MR, Bailey WL (2007) Results of the glucose-lowering effect of WelChol study (GLOWS): a randomized, double-blind, placebo-controlled pilot study evaluating the effect of colesevelam hydrochloride on glycemic control in subjects with type 2 diabetes. Clin Ther 29: 74–83.
40. Kajiyama G, Tazuma S, Yamashita G, Ochi H, Miura H, et al. (1996) Effect of MCI-196 on biliary lipids metabolism in patients with hypercholesterolemia. J Clin Ther Med 12: 1349–1359.
41. Garbutt JT, Kenney TJ (1972) Effect of cholestyramine on bile acid metabolism in normal man. J Clin Invest 51: 2781–2789.
42. Tomlinson E, Fu L, John L, Hultgren B, Huang X, et al. (2002) Transgenic mice expressing human fibroblast growth factor-19 display increased metabolic rate and decreased adiposity. Endocrinology 143: 1741–1747.
43. Katsuma S, Hirasawa A, Tsujimoto G (2005) Bile acids promote glucagon-like peptide-1 secretion through TGR5 in a murine enteroendocrine cell line STC-1. Biochem Biophys Res Commun 329: 386–390.
44. Kogire M, Gomez G, Uchida T, Ishizuka J, Greeley GH, Jr., et al. (1992) Chronic effect of oral cholestyramine, a bile salt sequestrant, and exogenous cholecystokinin on insulin release in rats. Pancreas 7: 15–20.
45. Koop I, Fellgiebel A, Koop H, Schafmayer A, Arnold R (1988) Effect of cholestyramine on plasma cholecystokinin and pancreatic polypeptide levels, and exocrine pancreatic secretion. Eur J Clin Invest 18: 517–523.
46. Shido O, Yoneda Y, Nagasaka T (1989) Changes in brown adipose tissue metabolism following intraventricular vasoactive intestinal peptide and other gastrointestinal peptides in rats. Jpn J Physiol 39: 359–369.
47. Yoshimatsu H, Egawa M, Bray GA (1992) Effects of cholecystokinin on sympathetic activity to interscapular brown adipose tissue. Brain Res 597: 298–303.
48. Brufau G, Bahr MJ, Staels B, Claudel T, Ockenga J, et al. (2010) Plasma bile acids are not associated with energy metabolism in humans. Nutr Metab (Lond) 7: 73.
49. Brufau G, Stellaard F, Prado K, Bloks VW, Jonkers E, et al. (2010) Improved glycemic control with colesevelam treatment in patients with type 2 diabetes is not directly associated with changes in bile acid metabolism. Hepatology 52: 1455–1464.

Original Article

Regression of Atherosclerosis in Apolipoprotein E-Deficient Mice is Feasible Using High-Dose Angiotensin Receptor Blocker, Candesartan

Kaori Hayashi, Hiroyuki Sasamura, Tatsuhiko Azegami and Hiroshi Itoh

Department of Internal Medicine, School of Medicine, Keio University, Tokyo, Japan

Aim: Clinical studies have suggested that renin-angiotensin inhibitors are effective for the prevention of atherosclerosis progression, but the results for the regression of established lesions are equivocal. The aim of this study was to examine the effects of different doses of the angiotensin receptor blocker (ARB) candesartan on the regression of atherosclerosis and lipid-induced nephropathy in apolipoprotein E (apoE)-deficient spontaneously hyperlipidemic (SHL) mice.

Methods and Results: Male SHL were given an atherogenic diet together with salt loading to induce atherosclerosis. The mice were then treated with various doses of candesartan (0-50 mg/kg/d) for 12 weeks. Treatment with high-dose candesartan caused clear regression of atherosclerotic plaques in the aorta, which was not observed with normal-dose candesartan. Biglycan and ACAT1 expression were significantly decreased, and aortic free cholesterol: cholesterol ester ratios were increased in these mice. Treatment of cultured THP-1 macrophages in vitro with candesartan resulted in a similar decrease in ACAT1 expression. In the kidney, glomerular lipid accumulation, mesangial expansion, and albuminuria were significantly regressed after treatment with high-dose candesartan, while biglycan and ACAT1 expressions were decreased.

Conclusion: These results suggest that regression of established atherosclerosis lesions in ApoE-deficient mice is feasible using high-dose candesartan, by mechanisms involving (i) a decrease in the lipid-retaining proteoglycan biglycan, and (ii) suppression of ACAT1 expression resulting in increased free cholesterol for lipid release.

J Atheroscler Thromb, 2012; 19:736-746.

Key words; Angiotensin receptor blocker, Candesartan, Regression, Biglycan, ACAT1

Introduction

Atherosclerosis is a leading cause of morbidity and mortality throughout the world[1]. Regression, or reversal of atherosclerotic lesions, could result in a marked decrease in coronary heart disease, stroke, and peripheral vascular disease[2, 3]; therefore, the development of methods for atherosclerosis regression represents an important therapeutic goal in the management of cardiovascular diseases.

Previous studies have suggested that the renin-angiotensin system (RAS) plays an important role in the onset and progression of atherosclerosis. Experimental studies have shown that treatment with RAS inhibitors prevents the formation of atherosclerotic lesions in animal models[4, 5]. Moreover, the use of angiotensin-converting enzyme (ACE) inhibitors and angiotensin receptor blockers (ARBs) has been shown in clinical studies to inhibit the progression of carotid medial thickening, decrease oxidative stress and inflammation, and improve endothelial function[6].

Interestingly, several preliminary studies have suggested that use of ARBs may cause a decrease or regression of plaque volumes. In an intravascular ultrasound study, Waseda *et al.* reported that treatment of patients with ARB was associated with a significant decrease in plaque volume[7]. Similar results were reported in the Multicenter Olmesartan atherosclero-

Address for correspondence: Hiroyuki Sasamura, Department of Internal Medicine, Keio University School of Medicine, 35 Shinanomachi, Shinjuku-ku, Tokyo 160-8582, Japan
E-mail: sasamura@a8.keio.jp
Received: November 11, 2011
Accepted for publication: February 21, 2012

sis Regression Evaluation (MORE) study, where plaque volume was assessed by non-invasive 2- and 3-dimensional ultrasound[8], as well as in other studies where atherosclerosis was assessed by evaluation of carotid intima-media thickness[9-11]. On the other hand, several other studies were unable to detect a significant effect of ARB on carotid intima-media thickness[12-14]. At present, the reasons for the discrepancies in the results of these clinical studies are unclear.

Recently, we reported that treatment of spontaneously hypertensive rats with high-dose ARB candesartan caused the reversal of renal arteriolar hypertrophy and regression of hypertension[15]. Similarly, high-dose candesartan, but not low-dose candesartan caused regression of glomerulosclerosis in adriamycin-treated mice[16]. These results suggest the possibility that the effects of candesartan on disease regression may require the use of high or ultra-high doses.

At present, it is unclear whether renin-angiotensin system blockade can cause the regression of fully established atherosclerotic lesions in mouse models of atherosclerosis. Moreover, the effects of different doses of candesartan on atherosclerotic lesions in ApoE-deficient mice have not been investigated. The aims of this study were therefore (i) to compare the effects of different doses of candesartan on established lesions of atherosclerosis and renal lesions in ApoE-deficient mice, and (ii) to examine potential mechanisms of these effects.

Materials and Methods

Animal Treatment Protocols

The studies were conducted using 4-week-old male spontaneously hyperlipidemic (SHL) mice (C57BL/6.KOR/StmSlc-*Apoe*^{shl}), which were obtained commercially from Sankyo Laboratory Service Corporation (Tokyo, Japan). All experiments were performed in accordance with the Animal Experimentation Guidelines of Keio University School of Medicine. Candesartan cilexetil (TCV-116) was a kind gift from Takeda Pharmaceutical Inc. (Tokyo, Japan).

SHL mice were divided into 6 groups as follows (n=8 per group): Group 1 was fed a normal rodent diet. Groups 2-6 were fed an atherogenic diet (15.0% lard and 0.15% cholesterol) obtained from Crea Japan (Tokyo, Japan), together with 1% NaCl in the drinking water for 12 weeks (from 5 to 16 weeks old). Group 2 was sacrificed at 16 weeks old before starting the ARB candesartan cilexetil treatment. Group 3, 4, 5 and 6 were treated for 12 weeks (from 16 to 28 weeks old) with ARB candesartan cilexetil was dissolved in the drinking water to deliver a dose of 0, 1, 10, 50 mg/kg/day, respectively, as described by us previously[15, 16]. All groups were returned to a normal diet with normal drinking water at age 16 weeks. Group 1 was sacrificed at 28 weeks old at the same time as Groups 3-6.

Biochemical Studies and Blood Pressure Measurement

Blood was collected by heart puncture after an overnight fast, centrifuged at 850 g for 15 min at 4℃, and stored at −20℃ until assay. Serum total cholesterol and HDL cholesterol were measured enzymatically. Urine collections were performed in metabolic cages, and urine albumin concentrations were determined by a direct competitive ELISA (Albuwell, Exocell, PA). Systolic blood pressures were estimated by indirect tail-cuff plethysmography using a Softron BP-98A manometer (Softron Inc., Tokyo, Japan). The protocol for blood pressure measurement was as follows: Preliminary blood pressure measurements were performed on two separate occasions to train the mice and to confirm that individual blood pressure variability was low. For the measurement of final blood pressures, the mean of 3-5 independent measurements was recorded at age 28 weeks, as recommended by the manufacturer.

Histological Analysis of Aortas and Kidneys

The heart and the aorta were immediately removed en bloc with a wide range of surrounding tissues. The aorta (from the ascending aorta to the abdominal aorta) was fixed in 4% paraformaldehyde, after which the whole aorta was opened longitudinally for en face Sudan IV staining. Sudan IV-positive areas in the aorta were quantified using Adobe Photoshop data analysis software (Adobe Systems, San Jose, CA, USA). For the assessment of atherosclerosis in the aortic root, heart sections containing the aortic root were fresh-frozen in OCT compound, and then sectioned using a cryotome prior to oil red O staining. For the assessment of renal injury, the kidneys were removed and fixed in 4% paraformaldehyde, and then embedded in paraffin blocks for periodic acid-Schiff (PAS) staining[16]. Other kidney samples for oil red staining and immunofluorescence analysis were fresh-frozen in OCT compound.

Immunofluorescence Staining and Western Blotting

Immunofluorescence staining and quantification of biglycan, ACAT1, and ABCA1 expression were performed on the cryostat sections using polyclonal anti-biglycan antibodies (Santa Cruz Biotechnology, Santa Cruz, CA, USA), polyclonal anti-ACAT1 antibodies

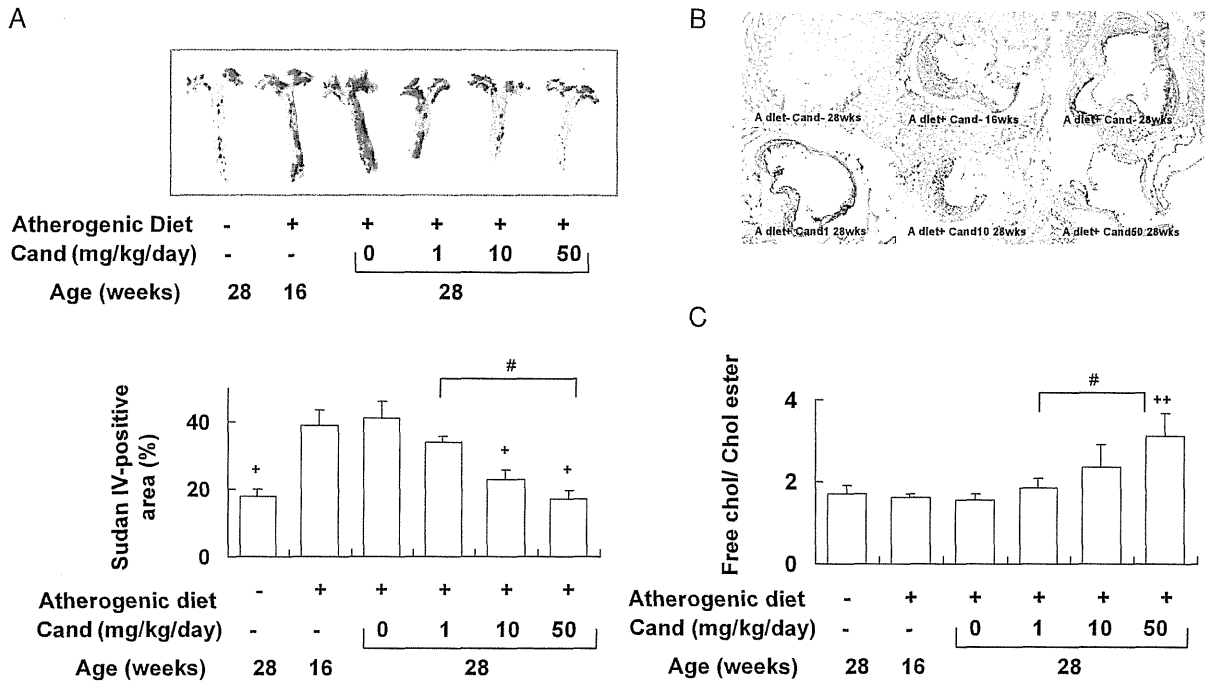

Fig. 1. Effects of different doses of candesartan on aortic atherosclerotic lesions of SHL mice induced by an atherogenic diet together with salt loading. (A) Upper panel: Representative photomicrographs of Sudan IV-stained aortas. Lower panel: Quantification of Sudan IV-positive areas as a percentage of whole aortic area. (B) Representative photomicrographs of oil red O-stained aortic roots. A diet: atherogenic diet, Cand: Candesartan. (C) The ratios of free cholesterol contents to cholesterol ester contents in the aortas of SHL mice. +: $p<0.05$, ++: $p<0.01$ vs atherogenic diet (+) Cand 0. #: $p<0.05$ vs the respective groups.

(Cayman Chemical, Ann Arbor, MI, USA), polyclonal anti-ABCA1 antibodies (Novus Biologicals, Littleton, CO, USA), monoclonal anti-CD68 antibodies (AbD Serotec, Oxford, UK), and polyclonal anti-apoB antibodies (Santa Cruz Biotechnology), as described previously[15, 16]. Western blotting for ACAT1 and ABCA1 in the aortas was performed as described by us previously[17]. Western blots were repeated on 4 samples from each group, and quantified using ImageQuant TL software (GE Healthcare, Buckinghamshire, UK), adjusting for the amount of alpha-tubulin (monoclonal anti-alpha-tubulin antibody, Sigma Aldrich, St Louis, MO, USA) as the housekeeping gene.

Lipid Extraction and Analysis

Total lipid was extracted from fresh-frozen samples of thoracic aortas or the renal cortex by the method of Bligh and Dyer[18, 19]. Total cholesterol and free cholesterol contents were measured using the cholesterol *E* test kit and free cholesterol *E* test kit (Wako Chemicals, Tokyo, Japan).

Cell Culture

The human monocytic leukemia cell line, THP-1 (obtained from DS Pharma Biomedical, Osaka, Japan) was grown in suspension culture in RPMI 1640 medium supplemented with 10% fetal bovine serum. To induce macrophage phenotype differentiation, phorbol 12-myristate 13-acetate (PMA, 100 ng/mL) was added to the culture medium to induce differentiation into macrophages[20, 21]. In some experiments, THP-1 cells were stimulated with 10 ug/mL oxidized LDL (ox-LDL; Cell Biolabs Inc., San Diego, CA, USA)[22, 23]. The differentiated macrophages were treated with candesartan (CV-11974, active metabolite of candesartan cilexetil, 10^{-6} mol/L) for 24 hours, and then ACAT1 and ABCA1 expressions were analyzed by Western blot analysis.

Statistics

Results are expressed as the mean ± SEM. Statistical comparisons were made by ANOVA followed by Scheffe's post-hoc test. $P<0.05$ was considered significant.

Table 1. Effects of ARB on body weight, systolic blood pressure, serum total cholesterol, and HDL-cholesterol in SHL mice

Atherogenic diet	−	+	+	+	+	+
Candesartan (mg/kg/day)	0	0	0	1	10	50
Age (weeks)	28	16	28	28	28	28
Body weight (g)	34.8±1.5	34.4±1.7	36.2±1.7	37.2±1.4	35.8±1.5	35.0±1.4
Systolic blood pressure (mmHg)	107.4±5.6	103.6±4.7	114±5.7	108.4±7.6	114.8±8.0	112.6±5.7
Total cholesterol (mg/dL)	528±96	540±198	613±62	497±17	620±113	588±62
HDL cholesterol (mg/dL)	15.0±4.5	16.4±2.4	13.0±2.0	17.0±1.2	13.8±2.4	13.0±3.0
Aortic cholesterol content (ng/mg)	273±46*	459±88	601±119	445±71	392±41	335±64*

*$p<0.05$ vs atherogenic diet (+) Candesartan 0, 28 weeks old

Results

Differential Effects of High-Dose Versus Normal-Dose ARB on Aortic Atherosclerotic Lesions of SHL Mice

SHL mice were fed an atherogenic diet with salt loading from 5 to 16 weeks of age. Mice in Group 2 were sacrificed at age 16 weeks, and lipid accumulation in the aorta and the aortic root were assessed by en face staining with Sudan IV and oil red O staining, respectively, to confirm that atherosclerosis had already developed at this age (**Fig. 1A, B**). Next, the effects of different doses of the ARB candesartan on atherosclerotic lesions were examined by treating the mice with candesartan from age 16 to age 28 weeks. It was found that treatment with candesartan at a normal dose (1 mg/kg/day in rodents[16]) for 12 weeks did not cause a significant change in the Sudan IV-stained area in the aorta. In contrast, treatment with high doses of candesartan (10 and 50 mg/kg/d) caused a significant decrease in aortic atherosclerotic lesions. Similar results were found for oil red O-stained areas in the aortic roots. Aortic cholesterol contents were also significantly decreased in high-dose ARB-treated mice. In contrast, no significant changes in systolic blood pressure, serum total cholesterol, or HDL-cholesterol were found in the different groups (**Table 1**). Furthermore, the free cholesterol: cholesterol ester ratios were significantly increased in the high-dose candesartan-treated group, but not in the normal-dose candesartan-treated group (**Fig. 1C**).

Effects of Different doses of ARB on Lipid-Related Factors in the Aorta of SHL Mice

To examine the possible role of the lipid-retaining proteoglycan biglycan in the regression of atherosclerosis, the expression of biglycan in the aortic plaques was examined by immunofluorescence staining. It was found that the expression of biglycan was significantly reduced by high-dose candesartan treatment, but not by low-dose candesartan, and a similar relation was seen with ApoB staining (**Fig. 2A**). Because the free cholesterol: cholesterol ester ratios were increased in candesartan-treated groups, we also examined ACAT1 expression in the different groups. As shown in **Fig. 2B**, the expression of ACAT1 was significantly decreased in the aortic plaques of candesartan-treated mice. In contrast, no significant differences were found in the expression of ATP-binding cassette transporter A1 (ABCA1) or for ABCG1 (data not shown). Double immunostaining revealed that biglycan expression co-localized with ApoB staining, and ACAT1 and ABCA1 were co-expressed with CD68-positive macrophages in the aortic plaques (**Fig. 2C**). The changes in ACAT1 and ABCA1 expression were confirmed by Western blotting (**Fig. 2D**). To confirm these actions of candesartan *in vitro*, we used the cultured human macrophage cell line THP-1, which was differentiated using the phorbol ester PMA. It was found that treatment with candesartan (10^{-6} M) induced a decreased expression of ACAT1 but not ABCA1. Similar results were found in THP-1 cells stimulated with ox-LDL (**Fig. 2E, F**).

Effects of Different doses of ARB on Glomerular Lesions in SHL Mice

Treatment of SHL mice with an atherogenic diet with salt loading from 5 to 16 weeks of age caused a significant increase in kidney glomerular lipid accumulation and mesangial expansion (**Fig. 3A-C**). Similar to the aorta, treatment with candesartan for 12 weeks caused a reduction in the number of oil red O-positive glomeruli, which was not statistically significant from the normal dose of candesartan (1 mg/kg/d), but was clearly seen with higher doses of candesartan (10 and 50 mg/kg/d). Quantitative assessment of the PAS-positive stained area revealed that the decrease in glomerular lipid accumulation was associated with a reduction in the mesangial matrix score in mice treated with higher doses of candesartan (10 and

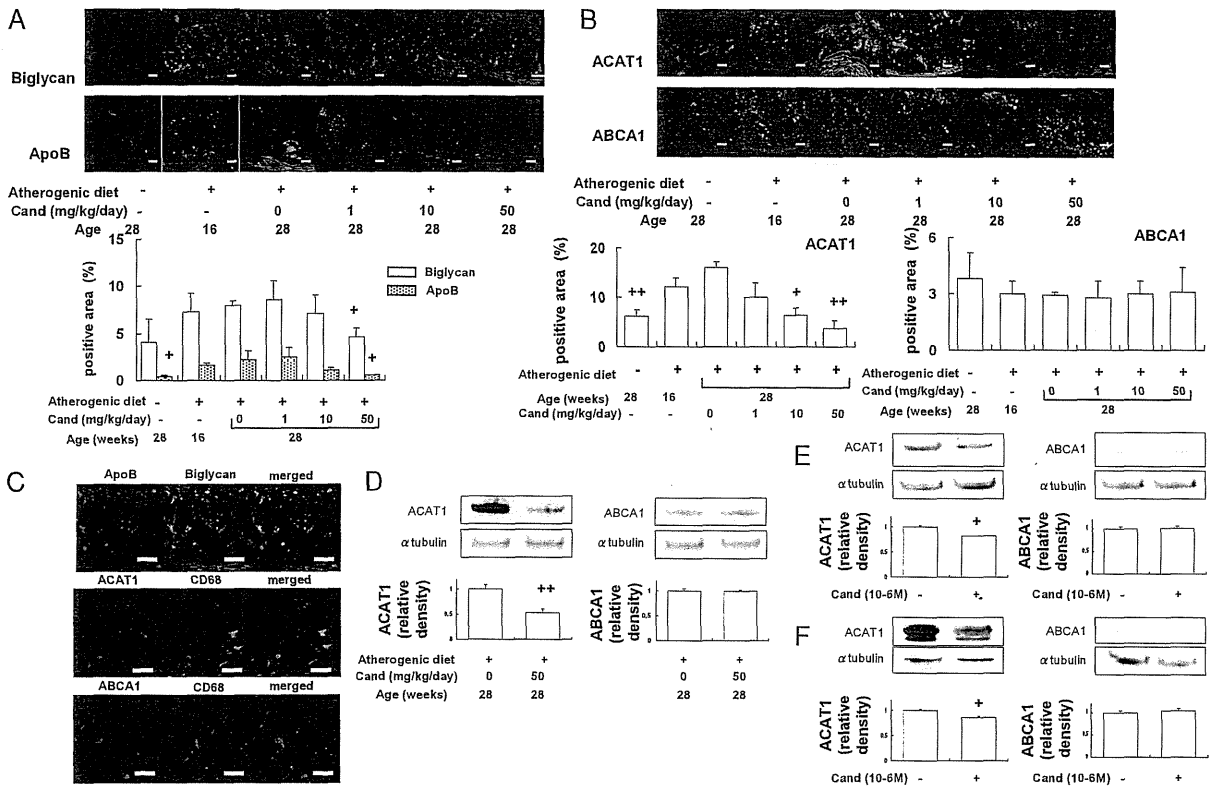

Fig. 2. Changes of lipid-related factors in the aortic atherosclerotic plaques of SHL mice with different doses of candesartan. (A) Representative photomicrographs of biglycan and ApoB immunofluorescence staining, and quantification of the stained area in the aortic plaques of SHL mice. (B) Representative photomicrographs of ACAT1 and ABCA1 immunofluorescence staining, and quantification of the stained area in the aortic plaques of SHL mice. (C) Representative dual immunofluorescence staining of biglycan (green) and apoB (red), CD68 (green) and ACAT1 (red) or ABCA1 (red) in the aortic plaques. (D) Western blotting for ACAT1 and ABCA1 in the aortas with or without high-dose candesartan treatment. (E) Western blotting for ACAT1 and ABCA1 in PMA-stimulated THP-1 cells with or without candesartan treatment for 24 h. (F) Western blotting for ACAT1 and ABCA1 in oxidized LDL-stimulated THP-1 cells with or without candesartan treatment for 24 h. Scale bar=20 um. Abbreviations as in Fig. 1.

50 mg/kg/d). Albuminuria was also significantly reduced in the high-dose candesartan-treated group (group 1: 58.8±11.5 mg/gCr, group 2: 67±31.5 mg/gCr, group 3: 101±30.7 mg/gCr, group 4: 63.9±21.7 mg/gCr, group 5: 51.9±22.2 mg/gCr, group 6: 37.5±9.1* mg/gCr, *$p<0.05$ vs group 3). The free cholesterol: total cholesterol ratios in the kidney were significantly increased in the high-dose candesartan-treated group, but not in the normal-dose candesartan-treated group (**Fig. 3D**).

Effects of Different doses of ARB on Lipid-Related Factors in the Kidney of SHL Mice

To investigate the potential mechanisms of these changes, the expressions of biglycan, ACAT1 and ABCA1 in the glomeruli were examined. As shown in **Fig. 4A, B**, the glomerular expression of biglycan and ACAT1 was significantly decreased in the high-dose candesartan-treated group, whereas the expression of ABCA1 was not significantly different between the groups, as in the aortic plaques. In the case of the renal glomeruli, both ACAT1 and ABCA1 expressions were found to be localized predominantly in the mesangial area, rather than CD68-positive macrophages (**Fig. 4C**).

Discussion

Atherosclerosis, which occurs as a result of excessive lipid accumulation in aortic plaques, is usually

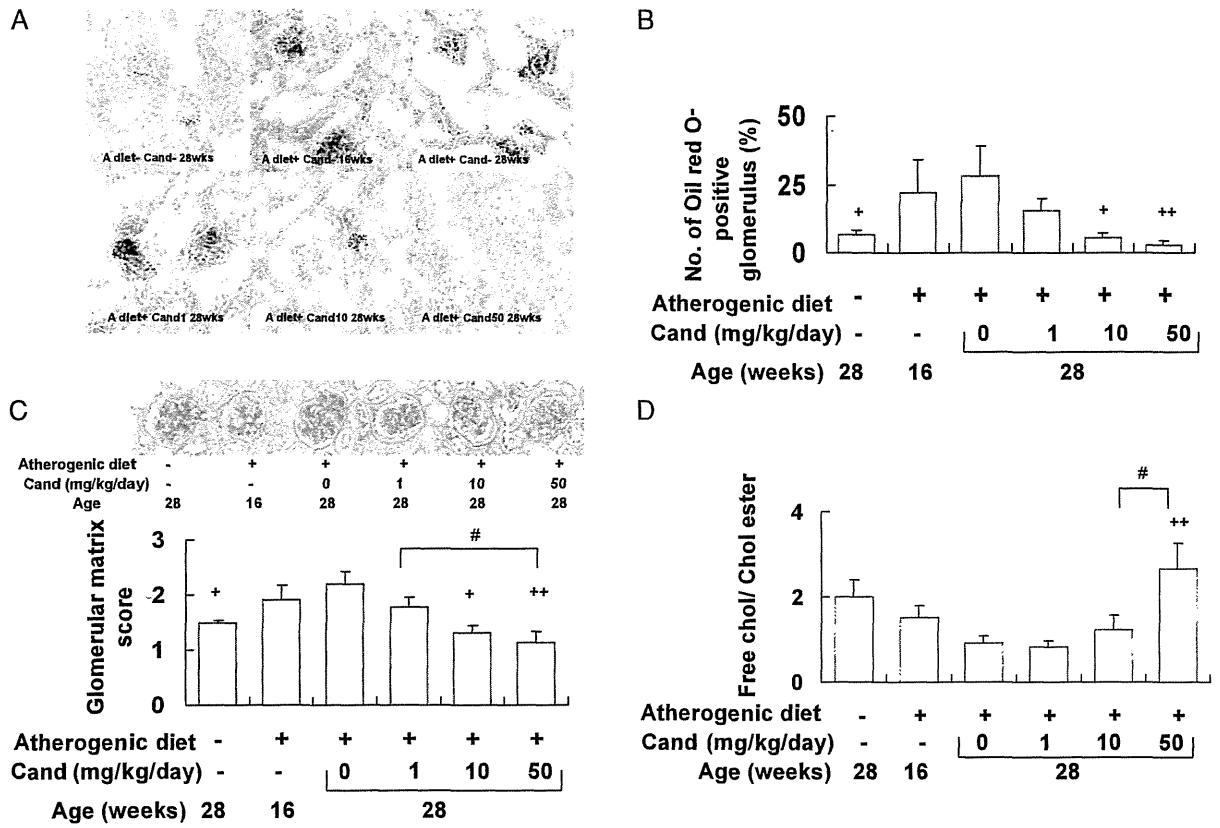

Fig. 3. Effects of different doses of candesartan on glomerular lesions of SHL mice induced by an atherogenic diet together with salt loading. (A) Representative photomicrographs of oil red O-stained kidney glomeruli (B) Quantification of oil red O-positive glomeruli as a percentage of total counted glomeruli. (C) Representative photomicrographs of glomerular histology, and quantification of glomerular matrix score. (D) Ratios of free cholesterol contents to cholesterol ester contents in the kidneys of SHL mice. Abbreviations as in Fig. 1.

considered a chronic and progressive process. Historically, the idea that atheromatous lesions may decrease in size has met with considerable resistance and skepticism[24, 25]; therefore, most previous pharmacological interventions have focused on the 'prevention' of atherosclerosis, that is, inhibition of the progression of atherosclerotic lesions. There have been fewer studies focusing on the mechanisms of 'regression', or the reversal of established atherosclerosis in animal models.

In one of the first studies on atherosclerosis regression, Friedman *et al.* treated cholesterol-fed rabbits with bolus injections of phosphatidylcholine and found a significant reduction in atheromatous plaques[26]. Recently, several clinical trials have examined the possible regression of atherosclerotic lesions in humans. Nissen *et al.* investigated the effects of recombinant ApoA-I Milano given intravenously for 5 weeks, and found a significant decrease in atheroma volume[27]. In the Reversal of Atherosclerosis with Aggressive Lipid Lowering (REVERSAL) study, the effect of high-dose statin therapy was compared with a conventional, less potent statin regimen. Patients treated with the conventional regimen exhibited a statistically significant progression of atheroma volume, whereas the high-dose statin group did not[28]. In the A Study to Evaluate the Effect of Rosuvastatin on Intravascular Ultrasound-Derived Coronary Atheroma Burden (ASTEROID) trial, all patients received high-dose statin therapy for 24 months, which resulted in a significant regression of coronary atherosclerosis[29]. The results of these studies suggest that the development of effective methods to cause the regression of atherosclerosis may be considered an achievable goal,

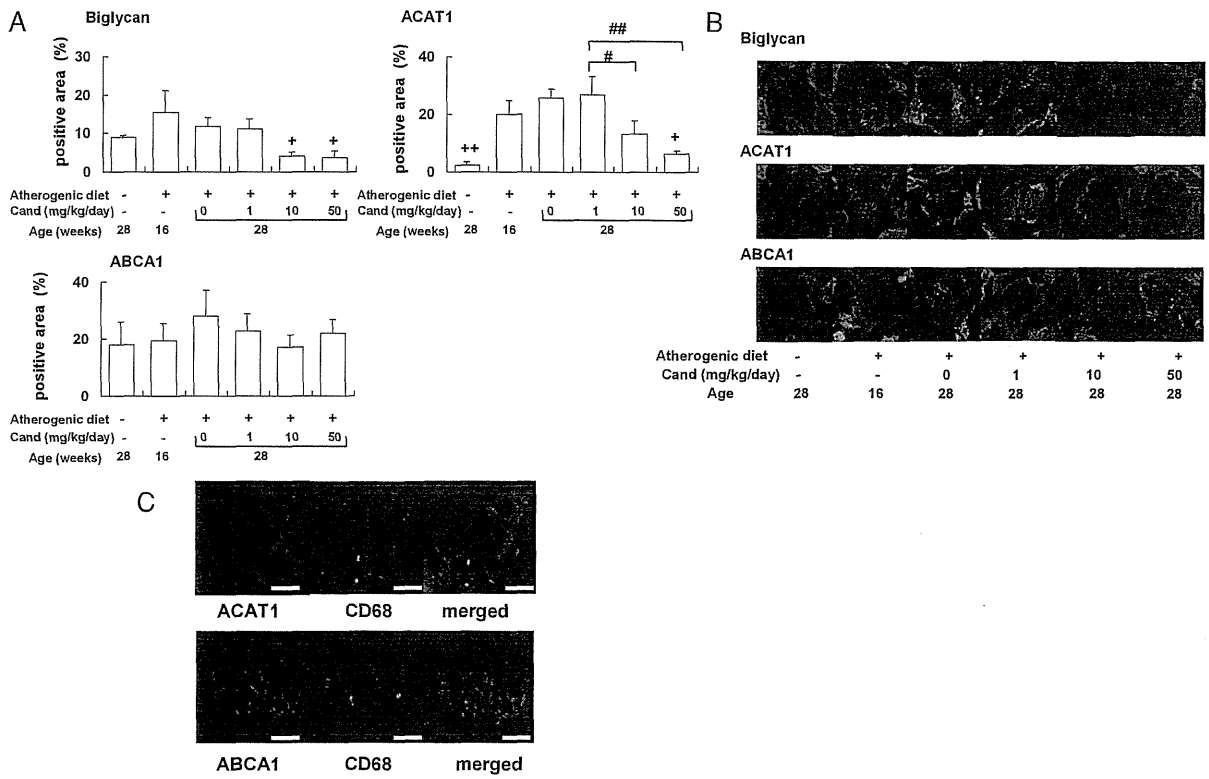

Fig. 4. Changes of lipid-related factors in the kidneys of SHL mice with different doses of candesartan. (A) Quantification of biglycan-, ACAT1- and ABCA1-stained areas in the glomeruli of SHL mice. (B) Representative photomicrographs of biglycan, ACAT1 and ABCA1 immunofluorescence staining. (C) Representative immunofluorescence staining of CD68 (green) and ACAT1 (red) or ABCA1 (red) in the kidneys of SHL mice with an atherogenic diet together with salt loading. Abbreviations as in Fig. 1.

in order to attenuate the growth in the increasing number of patients with cardiovascular diseases.

In this study, we compared the effect of different doses of the ARB candesartan on the regression of atherosclerosis in SHL mice. These SHL mice are known to have apoE gene mutations with more severe hypercholesterolemia and xanthoma, and generally milder atherosclerosis than apoE-null mice[30]. Preliminary experiments revealed that combining an atherogenic diet with salt loading in the drinking water resulted in the formation of severe atherosclerotic plaques in this model. Our results suggested that treatment for 12 weeks with high-dose candesartan resulted in the significant regression not only of aortic atherosclerotic lesions, but also of glomerular lipid deposits in the kidney.

It has been suggested that several mechanisms may contribute to atherosclerosis regression, including i) decreased retention of apoB lipoproteins within the arterial wall, and ii) efflux of cholesterol from plaques. Biglycan is a small leucine-rich proteoglycan which is expressed in the arterial wall and is thought to play a central role in the retention of atherogenic lipoproteins in atherosclerotic lesions[31]. We and others have shown that angiotensin II causes an increase in biglycan synthesis[32, 33], while treatment with ARB inhibits biglycan expression, which may contribute to the antiatherogenic effect of RAS inhibition[34, 35]. These reports suggest the possibility that the regression of atherosclerosis induced by high-dose candesartan treatment may be mediated by decreased biglycan expression, resulting in decreased accumulation of lipids in the arterial wall. In this study, we found that high-dose candesartan treatment caused a reduction of biglycan accumulation in both the aorta and the kidney glomeruli. The expression of biglycan was colocalized with ApoB expression in the aorta. In addition, a parallel relation was found between the expres-

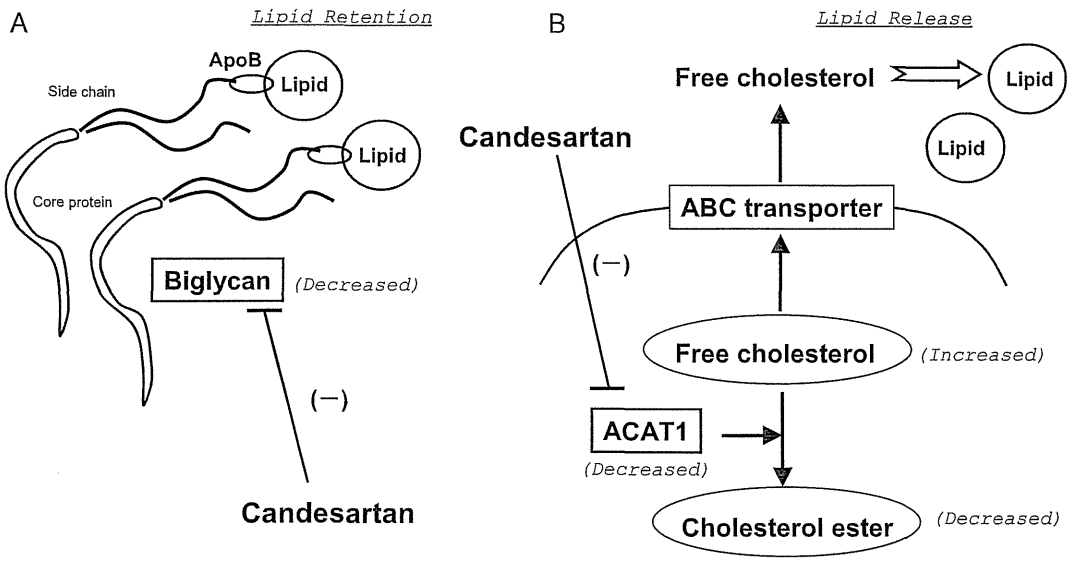

Fig. 5. Possible mechanisms of regression of atherosclerosis by high-dose candesartan treatment, involving (A) decreased lipid retention (B) increased lipid release.

sion of biglycan and ApoB with or without candesartan treatment. These results are consistent with the hypothesis that the decrease in biglycan expression was involved in the observed decrease in Oil Red-O-stained lipids in the aortic and glomerular lesions (**Fig. 5A**).

However, these results could not explain the finding that free cholesterol: cholesterol ester ratios were increased in the candesartan-treated groups; therefore, we next examined other mechanisms for the regression of atherosclerosis mediated by high-dose candesartan. ACAT1 is an intracellular enzyme that converts free cholesterol to cholesterol ester for storage in lipid droplets[36] (**Fig. 5B**). A decrease in ACAT1 expression causes decreased conversion from free cholesterol to cholesterol ester, resulting in the efflux of free cholesterol through ATP-binding cassette (ABC) transporters[37, 38], and removal from atherosclerotic plaques into HDL particles[39-41]. Moreover, several ACAT1 inhibitors achieved the regression of atherosclerotic lesions in animal models, mainly via an increase in the free cholesterol pool that is acceptable to HDL[42].

Recently, Kanome *et al.* demonstrated that angiotensin II upregulates ACAT1 expression by an AT1 receptor-dependent mechanism in cultured macrophages[43]. We therefore examined the hypothesis that candesartan treatment could cause changes in ACAT1 expression. We found that aortic ACAT1 expression was significantly lower than in control and standard-dose candesartan-treated groups, and the ratios of free cholesterol contents to cholesterol ester in high-dose candesartan-treated aortas were significantly higher. Moreover, treatment of cultured macrophages with candesartan resulted in a decrease in ACAT1 expression. Macrophages have been shown to induce the full expression of the components of the RAS, including the AT1 receptor[20]. These results are consistent with the possibility that candesartan treatment inhibits the action of locally generated angiotensin II, and therefore suppresses ACAT1 expression in macrophages.

Concerning the mechanisms of the effects of high-dose candesartan, it has been shown that maximal inhibition of the AT1 receptor is achieved at high concentrations of candesartan (1 uM or greater), which is higher than the plasma concentration achieved with normal-dose candesartan; therefore, the effects of high-dose candesartan could be explained by more complete inhibition of the AT1 receptor than with normal-dose candesartan. Interestingly, it has been shown that candesartan has multiple pleiotropic actions[44], some of which could be mediated by AT1 receptor-independent mechanisms[45]. The possibility that such mechanisms could contribute to the effects seen in this study cannot be completely ruled out.

Concerning the glomerular lipid deposits in hyperlipidemic mice, Wen *et al.* reported that glomerular lesions in ApoE-deficient mice were characterized

not only by lipid deposits, but also by increased deposition of glomerular matrix[46]. Similarly, Tomiyama-Hanayama *et al.* reported increased mesangial proliferation and matrix expansion in ApoE-deficient mice[47]. It has been reported that hyperlipidemia accelerates glomerulosclerosis, whereas manipulations to prevents intracellular lipid accumulation improve the progression of renal injury[48]. In our study, we found that lipid deposition, biglycan expression, and ACAT1/ABCA1 expression were predominantly co-localized to the mesangial area, and that candesartan treatment resulted in a decrease in lipid deposition. Therefore, high-dose candesartan treatment may have caused a decrease in mesangial lipid deposition by similar mechanisms as in the aortic macrophages, resulting in decreased mesangial expansion, and a significant reduction in albuminuria.

Concerning the dose of candesartan used in this study, candesartan has been shown to have an antihypertensive effect at 1 mg/kg/day in hypertensive rats[35] and hypertensive mice[49]. The dose of 50 mg/kg/day was 50 times the rodent antihypertensive dose; therefore, this was defined as 'high-dose' candesartan, as in our previous study[16]. In humans, the maximal antihypertensive dose in Japan is 12 mg/day. Interestingly, several studies have been performed to examine the effects of 'ultrahigh' doses of ARB (candesartan 16-128 mg/day or irbesartan 300-900 mg/day) in humans. The use of these high doses of ARB was associated with decreased proteinuria without dosage-related side effects[50, 51]; therefore, clinical use of high doses may be feasible. These studies also showed that the antiproteinuric effect of ARBs may be independent of the antihypertensive effect. In this study, the ARB candesartan had an antiatherogenic effect without a significant change in blood pressure, which is consistent with the notion that some actions of ARB may be mediated by blood pressure-independent mechanisms.

As mentioned in the introduction, several clinical studies have already suggested that use of ARBs may cause a decrease or regression of atherosclerosis[7, 8], but this has not been confirmed in other studies[12, 13]. To our knowledge, all previous clinical studies have been performed with a normal dose of ARB. In this study, we found that robust regression of atherosclerosis was only found in mice treated with high-dose ARB candesartan, suggesting that different doses may lead to different results.

In conclusion, the results of this study suggest that high-dose candesartan treatment causes regression of established atherosclerosis lesions in SHL mice, by mechanisms which may involve (i) decreased expression of the lipid-retaining proteoglycan biglycan, and (ii) reduced expression of the cholesterol converting enzyme ACAT1, resulting in a relative increase in free cholesterol for lipid release. These results may be important for designing therapies for the ultimate goal: to induce the regression of atherosclerotic disease and to substantially reduce stroke and coronary heart disease throughout the world.

Acknowledgements

The authors are grateful to Dr. Masataka Sata (Department of Cardiovascular Medicine, Institute of Health Biosciences, University of Tokushima Graduate School, Japan) and his collaborators at Tokyo University (Ms Yumi Kato and Ms Yumi Sugawara) for assistance with the quantitation of atherosclerotic plaques, to Dr. Shinji Kume (Department of Medicine, Shiga University of Medical Science, Japan) for assistance with kidney lipid quantitation, and Dr. Mitsuhiro Watanabe (Keio University) for helpful discussion about ACAT1 and ABCA1 expression.

Sources of Funding

This study was supported by a Grant-in-Aid for JSPS Fellows (2155542) and Grants for Scientific Research (20590984, 2155542, 20680105) from the Ministry of Education, Culture, Sports, Science and Technology (MEXT) of Japan, the Nateglinide Memorial Toyoshima Research and Education Fund, and the Salt Science Foundation, Tokyo, Japan.

Disclosures

None.

References

1) Libby P, Ridker PM, Hansson GK: Progress and challenges in translating the biology of atherosclerosis. Nature, 2011; 473: 317-325
2) Mangge H, Almer G, Truschnig-Wilders M, Schmidt A, Gasser R, Fuchs D: Inflammation, adiponectin, obesity and cardiovascular risk. Curr Med Chem, 2010; 17: 4511-4520
3) Charo IF, Taub R: Anti-inflammatory therapeutics for the treatment of atherosclerosis. Nat Rev Drug Discov, 2011; 10: 365-376
4) Montecucco F, Pende A, Mach F: The renin-angiotensin system modulates inflammatory processes in atherosclerosis: evidence from basic research and clinical studies. Mediators Inflamm, 2009; 2009: 752406
5) Sata M, Fukuda D: Crucial role of renin-angiotensin system in the pathogenesis of atherosclerosis. J Med Invest,

57: 12-25
6) Vaccari CS, Lerakis S, Hammoud R, Khan BV: Mechanisms of benefit of angiotensin receptor blockers in coronary atherosclerosis. Am J Med Sci, 2008; 336: 270-277
7) Waseda K, Ozaki Y, Takashima H, Ako J, Yasukawa T, Ismail TF, Hishida H, Ito T: Impact of angiotensin II receptor blockers on the progression and regression of coronary atherosclerosis: an intravascular ultrasound study. Circ J, 2006; 70: 1111-1115
8) Stumpe KO, Agabiti-Rosei E, Zielinski T, Schremmer D, Scholze J, Laeis P, Schwandt P, Ludwig M: Carotid intima-media thickness and plaque volume changes following 2-year angiotensin II-receptor blockade. The Multicentre Olmesartan atherosclerosis Regression Evaluation (MORE) study. Ther Adv Cardiovasc Dis, 2007; 1: 97-106
9) Ono H, Minatoguchi S, Watanabe K, Yamada Y, Mizukusa T, Kawasaki H, Takahashi H, Uno T, Tsukamoto T, Hiei K, Fujiwara H: Candesartan decreases carotid intima-media thickness by enhancing nitric oxide and decreasing oxidative stress in patients with hypertension. Hypertens Res, 2008; 31: 271-279
10) Ludwig M, Stapff M, Ribeiro A, Fritschka E, Tholl U, Smith RD, Stumpe KO: Comparison of the effects of losartan and atenolol on common carotid artery intima-media thickness in patients with hypertension: results of a 2-year, double-blind, randomized, controlled study. Clin Ther, 2002; 24: 1175-1193
11) Mortsell D, Malmqvist K, Held C, Kahan T: Irbesartan reduces common carotid artery intima-media thickness in hypertensive patients when compared with atenolol: the Swedish Irbesartan Left Ventricular Hypertrophy Investigation versus Atenolol (SILVHIA) study. J Intern Med, 2007; 261: 472-479
12) Tomas JP, Moya JL, Barrios V, Campuzano R, Guzman G, Megias A, Ruiz-Leria S, Catalan P, Marfil T, Tarancon B, Muriel A, Garcia-Lledo A: Effect of candesartan on coronary flow reserve in patients with systemic hypertension. J Hypertens, 2006; 24: 2109-2114
13) Kosch M, Levers A, Lang D, Bartels V, Rahn KH, Pavenstadt H, Hausberg M: A randomized, double-blind study of valsartan versus metoprolol on arterial distensibility and endothelial function in essential hypertension. Nephrol Dial Transplant, 2008; 23: 2280-2285
14) Okura T, Watanabe S, Kurata M, Koresawa M, Irita J, Enomoto D, Jotoku M, Miyoshi K, Fukuoka T, Higaki J: Long-term effects of angiotensin II receptor blockade with valsartan on carotid arterial stiffness and hemodynamic alterations in patients with essential hypertension. Clin Exp Hypertens, 2008; 30: 415-422
15) Ishiguro K, Hayashi K, Sasamura H, Sakamaki Y, Itoh H: "Pulse" treatment with high-dose angiotensin blocker reverses renal arteriolar hypertrophy and regresses hypertension. Hypertension, 2009; 53: 83-89
16) Hayashi K, Sasamura H, Ishiguro K, Sakamaki Y, Azegami T, Itoh H: Regression of glomerulosclerosis in response to transient treatment with angiotensin II blockers is attenuated by blockade of matrix metalloproteinase-2. Kidney international, 2010; 78: 69-78
17) Kobayashi E, Sasamura H, Mifune M, Shimizu-Hirota R, Kuroda M, Hayashi M, Saruta T: Hepatocyte growth factor regulates proteoglycan synthesis in interstitial fibroblasts. Kidney international, 2003; 64: 1179-1188
18) Bligh EG, Dyer WJ: A rapid method of total lipid extraction and purification. Can J Biochem Physiol, 1959; 37: 911-917
19) Kume S, Uzu T, Araki S, Sugimoto T, Isshiki K, Chin-Kanasaki M, Sakaguchi M, Kubota N, Terauchi Y, Kadowaki T, Haneda M, Kashiwagi A, Koya D: Role of altered renal lipid metabolism in the development of renal injury induced by a high-fat diet. J Am Soc Nephrol, 2007; 18: 2715-2723
20) Okamura A, Rakugi H, Ohishi M, Yanagitani Y, Takiuchi S, Moriguchi K, Fennessy PA, Higaki J, Ogihara T: Upregulation of renin-angiotensin system during differentiation of monocytes to macrophages. J Hypertens, 1999; 17: 537-545
21) Daigneault M, Preston JA, Marriott HM, Whyte MK, Dockrell DH: The identification of markers of macrophage differentiation in PMA-stimulated THP-1 cells and monocyte-derived macrophages. PloS one, 2010; 5: e8668
22) McLaren JE, Michael DR, Guschina IA, Harwood JL, Ramji DP: Eicosapentaenoic Acid and Docosahexaenoic Acid Regulate Modified LDL Uptake and Macropinocytosis in Human Macrophages. Lipids, 2011; 46: 1053-1061
23) Inoue M, Itoh H, Tanaka T, Chun TH, Doi K, Fukunaga Y, Sawada N, Yamshita J, Masatsugu K, Saito T, Sakaguchi S, Sone M, Yamahara K, Yurugi T, Nakao K: Oxidized LDL regulates vascular endothelial growth factor expression in human macrophages and endothelial cells through activation of peroxisome proliferator-activated receptor-gamma. Arteriosclerosis, thrombosis, and vascular biology, 2001; 21: 560-566
24) Shanmugam N, Roman-Rego A, Ong P, Kaski JC: Atherosclerotic plaque regression: fact or fiction? Cardiovasc Drugs Ther, 24: 311-317
25) Williams KJ, Feig JE, Fisher EA: Rapid regression of atherosclerosis: insights from the clinical and experimental literature. Nat Clin Pract Cardiovasc Med, 2008; 5: 91-102
26) Friedman M, Byers SO, Rosenman RH: Resolution of aortic atherosclerotic infiltration in the rabbit by phosphatide infusion. Proc Soc Exp Biol Med, 1957; 95: 586-588
27) Nissen SE, Tsunoda T, Tuzcu EM, Schoenhagen P, Cooper CJ, Yasin M, Eaton GM, Lauer MA, Sheldon WS, Grines CL, Halpern S, Crowe T, Blankenship JC, Kerensky R: Effect of recombinant ApoA-I Milano on coronary atherosclerosis in patients with acute coronary syndromes: a randomized controlled trial. Jama, 2003; 290: 2292-2300
28) Nissen SE, Tuzcu EM, Schoenhagen P, Brown BG, Ganz P, Vogel RA, Crowe T, Howard G, Cooper CJ, Brodie B, Grines CL, DeMaria AN: Effect of intensive compared with moderate lipid-lowering therapy on progression of coronary atherosclerosis: a randomized controlled trial. Jama, 2004; 291: 1071-1080
29) Nissen SE, Nicholls SJ, Sipahi I, Libby P, Raichlen JS, Ballantyne CM, Davignon J, Erbel R, Fruchart JC, Tardif

JC, Schoenhagen P, Crowe T, Cain V, Wolski K, Goormastic M, Tuzcu EM: Effect of very high-intensity statin therapy on regression of coronary atherosclerosis: the ASTEROID trial. Jama, 2006; 295: 1556-1565
30) Matsushima Y, Hayashi S, Tachibana M: Spontaneously hyperlipidemic (SHL) mice: Japanese wild mice with apolipoprotein E deficiency. Mamm Genome, 1999; 10: 352-357
31) Nakashima Y, Wight TN, Sueishi K: Early atherosclerosis in humans: role of diffuse intimal thickening and extracellular matrix proteoglycans. Cardiovasc Res, 2008; 79: 14-23
32) Huang F, Thompson JC, Wilson PG, Aung HH, Rutledge JC, Tannock LR: Angiotensin II increases vascular proteoglycan content preceding and contributing to atherosclerosis development. J Lipid Res, 2008; 49: 521-530
33) Shimizu-Hirota R, Sasamura H, Kuroda M, Kobayashi E, Hayashi M, Saruta T: Extracellular matrix glycoprotein biglycan enhances vascular smooth muscle cell proliferation and migration. Circ Res, 2004; 94: 1067-1074
34) Nagy N, Melchior-Becker A, Fischer JW: Long-term treatment with the AT1-receptor antagonist telmisartan inhibits biglycan accumulation in murine atherosclerosis. Basic Res Cardiol, 2010; 105: 29-38
35) Sasamura H, Shimizu-Hirota R, Nakaya H, Saruta T: Effects of AT1 receptor antagonist on proteoglycan gene expression in hypertensive rats. Hypertens Res, 2001; 24: 165-172
36) Lei X, Fujiwara Y, Chang CC, Chang TY, Takeya M, Sakashita N: Association of ACAT1-positive vesicles with late endosomes/lysosomes in cholesterol-rich human macrophages. Journal of atherosclerosis and thrombosis, 2010; 17: 740-750
37) Pagler TA, Wang M, Mondal M, Murphy AJ, Westerterp M, Moore KJ, Maxfield FR, Tall AR: Deletion of ABCA1 and ABCG1 impairs macrophage migration because of increased Rac1 signaling. Circ Res, 2011; 108: 194-200
38) Sekiya M, Osuga JI, Igarashi M, Okazaki H, Ishibashi S: The Role of Neutral Cholesterol Ester Hydrolysis in Macrophage Foam Cells. Journal of atherosclerosis and thrombosis, 2011;
39) Lee RG, Willingham MC, Davis-MA, Skinner KA, Rudel LL: Differential expression of ACAT1 and ACAT2 among cells within liver, intestine, kidney, and adrenal of nonhuman primates. J Lipid Res, 2000; 41: 1991-2001
40) Chang TY, Li BL, Chang CC, Urano Y: Acyl-coenzyme A: cholesterol acyltransferases. Am J Physiol Endocrinol Metab, 2009; 297: E1-9
41) Rudel LL, Lee RG, Cockman TL: Acyl coenzyme A: cholesterol acyltransferase types 1 and 2: structure and function in atherosclerosis. Curr Opin Lipidol, 2001; 12: 121-127
42) Rodriguez A, Bachorik PS, Wee SB: Novel effects of the acyl-coenzyme A: Cholesterol acyltransferase inhibitor 58-035 on foam cell development in primary human monocyte-derived macrophages. Arteriosclerosis, thrombosis, and vascular biology, 1999; 19: 2199-2206
43) Kanome T, Watanabe T, Nishio K, Takahashi K, Hongo S, Miyazaki A: Angiotensin II upregulates acyl-CoA: cholesterol acyltransferase-1 via the angiotensin II Type 1 receptor in human monocyte-macrophages. Hypertens Res, 2008; 31: 1801-1810
44) Koh KK, Ahn JY, Han SH, Kim DS, Jin DK, Kim HS, Shin MS, Ahn TH, Choi IS, Shin EK: Pleiotropic effects of angiotensin II receptor blocker in hypertensive patients. Journal of the American College of Cardiology, 2003; 42: 905-910
45) Chen S, Ge Y, Si J, Rifai A, Dworkin LD, Gong R: Candesartan suppresses chronic renal inflammation by a novel antioxidant action independent of AT1R blockade. Kidney international, 2008; 74: 1128-1138
46) Wen M, Segerer S, Dantas M, Brown PA, Hudkins KL, Goodpaster T, Kirk E, LeBoeuf RC, Alpers CE: Renal injury in apolipoprotein E-deficient mice. Lab Invest, 2002; 82: 999-1006
47) Tomiyama-Hanayama M, Rakugi H, Kohara M, Mima T, Adachi Y, Ohishi M, Katsuya T, Hoshida Y, Aozasa K, Ogihara T, Nishimoto N: Effect of interleukin-6 receptor blockage on renal injury in apolipoprotein E-deficient mice. Am J Physiol Renal Physiol, 2009; 297: F679-684
48) Abrass CK: Cellular lipid metabolism and the role of lipids in progressive renal disease. Am J Nephrol, 2004; 24: 46-53
49) Hirono Y, Yoshimoto T, Suzuki N, Sugiyama T, Sakurada M, Takai S, Kobayashi N, Shichiri M, Hirata Y: Angiotensin II receptor type 1-mediated vascular oxidative stress and proinflammatory gene expression in aldosterone-induced hypertension: the possible role of local renin-angiotensin system. Endocrinology, 2007; 148: 1688-1696
50) Rossing K, Schjoedt KJ, Jensen BR, Boomsma F, Parving HH: Enhanced renoprotective effects of ultrahigh doses of irbesartan in patients with type 2 diabetes and microalbuminuria. Kidney international, 2005; 68: 1190-1198
51) Burgess E, Muirhead N, Rene de Cotret P, Chiu A, Pichette V, Tobe S: Supramaximal dose of candesartan in proteinuric renal disease. J Am Soc Nephrol, 2009; 20: 893-900

Molecular and Cellular Endocrinology 365 (2013) 36–43

Contents lists available at SciVerse ScienceDirect

Molecular and Cellular Endocrinology

journal homepage: www.elsevier.com/locate/mce

Identification of endocrine disrupting chemicals activating SXR-mediated transactivation of *CYP3A* and *CYP7A1*

Tingting Zhou [a,1], Shuyan Cong [b,1], Shiying Sun [a], Hongmiao Sun [a], Renlong Zou [a], Shengli Wang [a], Chunyu Wang [a], Jiao Jiao [a], Kiminobu Goto [c], Hajime Nawata [d], Toshihiko Yanase [e], Yue Zhao [a,*]

[a] *Department of Cell Biology, Key Laboratory of Cell Biology, Ministry of Public Health of China, China Medical University, No. 92 Beier Road, Shenyang 110001, China*
[b] *Department of Neurology, Shengjing Hospital of China Medical University, Sanhao Street 36, Shenyang 110003, China*
[c] *Department of Medicine and Bioregulatory Science (3rd Department of Internal Medicine), Graduate School of Medical Sciences, Kyushu University, Maidashi 3-1-1, Higashi-ku, Fukuoka 812-8582, Japan*
[d] *Fukuoka Prefectural University, Tagawa City, Fukuoka 825-8585, Japan*
[e] *Department of Endocrinology and Diabetes Mellitus, School of Medicine, Fukuoka University, 7-45-1 Nanakuma, Jonan-ku, Fukuoka 814-0180, Japan*

ARTICLE INFO

Article history:
Received 23 March 2012
Received in revised form 3 September 2012
Accepted 3 September 2012
Available online 10 September 2012

Keywords:
Endocrine disrupting chemicals
SXR
CYP3A
CYP7A1
Xenobiotic metabolism

ABSTRACT

Endocrine disrupting chemicals (EDCs) have emerged as a major public health issue because of their potentially disruptive effects on physiological hormonal actions. SXR (steroid xenobiotic receptor), also known as NR1I2, regulates *CYP3A* expression in response to exogenous chemicals, such as EDCs, after binding to SXRE (SXR response element). In our study, luciferase assay showed that 14 out of 55 EDCs could enhance SXR-mediated rat or human *CYP3A* gene transcription nearly evenly, and could also activate rat *CYP7A1* gene transcription by cross-interaction of SXR and LXRE (LXRα response element). SXR diffused in the nucleus without ligand, whereas intranuclear foci of liganded SXR were produced. Furthermore, endogenous mRNA expression of *CYP3A4* gene was enhanced by the 14 positive EDCs. Our results suggested a probable mechanism of EDCs disrupting the steroid or xenobiotic metabolism homeostasis via SXR.

1. Introduction

Endocrine disrupting chemicals or environmental endocrine disrupters (EDCs), which are compounds appearing in environment, including pharmaceutical agents, pesticides and their byproducts, etc., are found to interfere with metabolism or signaling of normal hormone (Diamanti-Kandarakis et al., 2009). As many EDCs mimic the action of sex hormones, they have emerged as a major public health issue because of their potentially disruptive effects on physiological hormonal actions, such as steroidogenesis, particularly through direct interaction with estrogen receptor (ER) (Craig et al., 2011; Hall and Korach, 2002) or on male sex development by associating with androgen receptor (AR) (Fang et al., 2003). Increasing studies tend to link exposure to EDCs and hormone-dependent cancer risks, such as breast cancer and prostate cancer (Mnif et al., 2011).

A family of cytochrome P450 enzymes (CYPs) metabolizes endogenous steroid hormones as well as exogenous compounds such as drugs or EDCs. The transcriptional regulation of such CYP genes is mediated by "orphan" nuclear receptor subfamily members, designated human steroid xenobiotic receptor (SXR), liver X receptor (LXR), farnesol X receptor (FXR) or peroxisome proliferater activator receptor (PPAR). They form heterodimers with retinoid X receptor (RXR) to bind to response elements named SXRE, LXRE, FXRE, and PPRE, respectively. These response elements consist of repeat of the core consensus sequence AGGTCA spaced by 1 to 6 nucleotides, and thus both the orientation of each core sequence and the number of spacing nucleotides control the binding specificity of each receptor (Waxman, 1999; Edwards et al., 2002; Blumberg and Evans, 1998; Lehmann et al., 1997).

The nuclear receptor SXR, which induces *CYP3A* genes transcription, was also named as NR1I2 or pregnane activated receptor (PAR) (Blumberg et al., 1998; Bertilsson et al., 1998). The rodent homologue of SXR is pregnane X receptor (PXR) Xie et al., 2000.

Abbreviations: EDCs, endocrine disrupting chemicals/environmental endocrine disrupters; SXR, steroid xenobiotic receptor in human; PXR, pregnane X receptor in rodent (rodent homologue of SXR); PAR, pregnane activated receptor; LXRα, liver X receptor alpha; FXR, farnesol X receptor; PPAR, peroxisome proliferator activator receptor; RXR, retinoid X receptor; SXRE/PXRE/LXRE/PPRE, SXR/PXR/LXRα/the peroxisome proliferator response element; DR3, PXRE in the promoter region of rat *CYP3A2* gene; ER6, SXRE in the promoter region of human *CYP3A4* gene; βDR4, LXRE in the promoter region of rat *CYP7A1* gene; ER, estrogen receptor; AR, androgen receptor; GR, glucocorticoid receptor.

* Corresponding author. Address: Laboratory of Chromatin Biology, Department of Cell Biology, Key Laboratory of Cell Biology, Education Ministry, Ministry of Public Health of China, China Medical University, No. 92 Beier Road, Shenyang 110001, China. Tel.: +86 24 23256666 6010; fax: +86 24 23269606.
E-mail address: zhaoyue@mail.cmu.edu.cn (Y. Zhao).
[1] These authors contributed equally to this work.

0303-7207/$ - see front matter © 2012 Elsevier Ireland Ltd. All rights reserved.
http://dx.doi.org/10.1016/j.mce.2012.09.001

CYP3As play vital roles in metabolism of a variety of endogenous substrates such as steroids, bile acids and retinoic acid (Masuyama et al., 2000). Moreover, CYP3As are involved in catabolization and detoxication of plentiful exogenous chemicals, and they are important for clearance of nearly 60% of clinically administered drugs, such as anticancer drugs (Lehmann et al., 1998; Masuyama et al., 2007; Raynal et al., 2010). The predominant form of CYP3A is CYP3A2 in rodent or CYP3A4 in human, while it has been shown that the spectrum of drug metabolism is different among species (Waxman, 1999). Furthermore, SXR was shown to influence the clinical efficacy of anticancer drugs (Masuyama et al., 2007; Raynal et al., 2010).

SXR is unique, since it binds to many chemicals, including natural steroids, such as pregnenolone, dehydroepiandrosterone, corticosterone and synthetic chemicals such as rifampicin, dexamethasone (glucocorticoid) and pregnenolone 16α-carbonitrile (antiglucocorticoid) (Blumberg et al., 1998; Xie et al., 2000; Kliewer and Willson, 2002). The affinities of these compounds to SXR are remarkably low (10^{-6}–10^{-5}M of ligand concentration) when compared with classic steroid hormone receptors. By studying PXR knockout animal models, PXR was also found to mediate the transcription of rat *CYP7A1* (cholesterol 7α-hydroxylase) gene (Staudinger et al., 2001). SXR plays an important role in cholesterol metabolism (Sonoda et al., 2005) and lipid homeostasis (Roth et al., 2008).

So far, some EDCs have been shown to bind to SXR and modulate the activity of SXR by affecting transcription of SXR target genes (Mikamo et al., 2003; Lemaire et al., 2004). It was mentioned that EDCs, including nonylphenol, increased the mRNA level of *CYP3A1* by stimulating SXR, suggesting a possible role of EDCs in the function of altering steroid hormone metabolism via CYP3A1 regulation (Masuyama et al., 2000). Furthermore, nonylphenol was found to activate PXR and induce P450 enzymes to increase the production of estriol (E3), which in turn increased mammary cancer incidence in the MMTVneu mouse model (Acevedo et al., 2005). In the current study, from 55 environmental compounds, we identified 14 positive EDCs, which were able to activate SXR-induced transactivation of *CYP3A2, CYP3A4* and *CYP7A1* gene. Moreover, we intended to provide evidence for the potential relationship between EDCs and steroid or xenobiotic metabolism homeostasis via SXR.

2. Materials and methods

2.1. Chemicals

Natural steroids and chemicals suspected to possess the activities as EDCs were purchased from Wako Pure Chemical Industries, Ltd. (Osaka, Japan) according to the guidelines of the company and the Ministry of International Trade and Industry. Troglitazone was kindly provided by Daiichi Sankyo, and rifampicin was purchased from Sigma.

2.2. Cells

CV-1 cells and HepG2 cells were obtained from the Riken Cell Bank (Tokyo). Cells were maintained in DMEM (Life Technologies), supplemented with 10% FBS, 2 mM of L-Glutamine. For transfection experiments, cells were inoculated in dishes with DMEM containing 10% coal-treated FBS for 16 h before transfection, and then were treated with or without EDCs.

2.3. Plasmids constructs

A plasmid expressing SXR (pHSXR) was created by inserting a full length cDNA fragment of SXR, amplified by PCR (Advantage cDNA Polymerase Mix, Clontech) using Human Liver Marathon-Ready cDNA (Clontech) as a template, into an expression vector plasmid pcDNA3(+). Kozak translational start site (CCATGG) was engineered into 5′ end of SXR to provide strong initiation methionine. In the same manner, full length of the coding sequence of SXR was ligated into pECFP (Clontech) to create plasmid pECFP-SXR expressing chimeric SXR protein fused at its C-terminus to N-terminus of cyan fluorescence protein (CFP). A reporter plasmid, ptkCYPDR3×3luc, ptkCYPER6×3luc, or ptkCYPβDR4×3luc was created by ligating 3 copies of a PXRE, an SXRE or a rat LXRE sequence into pGL3tk-luc vector. The reporter sequence includes a PXRE sequence in *CYP3A2* (Kliewer and Willson, 2002), an SXRE sequence in *CYP3A4* (Lehmann et al., 1998), or an LXRE sequence in rat *CYP7A1* (Willy et al., 1995), respectively (Table 2). pGL3tk-luc was created by inserting HSV-TK promoter sequence [BglII/HindIII fragment of pRL-TK vector (Promega Corporation)] into BglII/HindIII pGL3-basic vector. The validity of each plasmid construct was confirmed by sequencing of the insert using ABIPRISM377 DNA Sequencer (Perkin Elmer, Norwalk C-T, USA), and for pHSXR, the expressed protein in bacteria was subjected to SDS–PAGE to confirm the correct molecular weight of SXR.

2.4. Luciferase assay

5×10^5 CV-1 cells/well were transfected using Lipofectamine (GIBCO BRL) with 1.6 μg/well of reporter plasmid ptkCYPDR3×3luc, ptkCYPER6×3luc, or ptkCYPβDR4×3luc, and 0.8 μg/well of pHSXR expressing SXR. pRL-CMV vector was used as an internal control. 4 h after transfection, the cells were rinsed and incubated in DMEM supplemented with 10% coal-treated FBS. At 16 h posttransfection, the cells were separated into 96 well dishes, and then were treated with negative control (ethanol), 5×10^{-6} M of positive control (corticosterone, rifampicin, troglitozone) or 55 EDCs (Table 1) for 16 h to identify the positive EDCs for SXR. Similar experiments were performed as above for dose-dependent luciferase assay with 5×10^{-8}, 5×10^{-7}, 5×10^{-6}, 5×10^{-5} M of indicated compounds. After 36 h posttransfection, the cells were harvested and assayed for luciferase activities by using a Dual-luciferase reporter assay system (Promega) as previous experiments (Zhao et al., 2009). All experiments were repeated at least 4 times with the independently prepared plasmid samples. The data are presented as the means ± SD.

2.5. Subcellular localization of human SXR in CV-1 cells

CV-1 cells were divided into 35 mm glass-bottom dishes (MatTek Corporation) and then were transfected with pECFP-SXR. 4 h after transfection, the cells were rinsed and incubated in DMEM supplemented with 10% coal-treated FBS in the absence or presence of corticosterone, rifampicin and benzo(a)pyrene (5×10^{-6} M). After additional 20 h, the cell nuclei were stained with TOPRO3 and the cells were scanned using confocal laser scanning microscopy (Leica TCS-SP system, Leica Microsystems, Heidelberg, Germany). The cells were imaged for cyan fluorescence by excitation with the 458 nm line of an argon laser, and the emission was viewed through a 470–500 nm band pass filter. The nuclei were imaged for TOPRO3 fluorescence by excitation of 642 nm and emission of 661 nm.

2.6. CYP3A4 mRNA expression

HepG2 cells were cultured in DMEM with 10% coal-treated FBS in the presence of ethanol, corticosterone, rifampicin, troglitozone, and 15 EDCs (5×10^{-6} M) shown in Fig. 1. 48 h after administration, total RNA was isolated using the Trizol reagent (Invitrogen). Reverse transcription was performed using SuperScript II

Table 1
A list of 55 chemicals, which were suspected to possess endocrine disrupting chemicals (EDCs) activity, was classified by their application.

Herbicides	**Insecticides**	
Alachlor	Aldicard	Endrin
Amitrole	Aldrin	Esfenvalerate
Atrazine	Carbaryl (NAC)	Fenvalerate (FEN)
2,4-Dichlorophenol (2,4-DCP)	trans-Chlordane	Heptachlor
2,4-Dichlorophenoxy acetic acid	cis-Chlordane	β-Hexachlorocyclohexane
Hexachlorobenzen	Cypermethrin	γ-Hexachlorocyclohexane
Metribuzin	*p,p'*-DDD	Kelthane (KEL)
Nitrofen	*p,p'*-DDE	Malathion
Pentachlorophenol	*p,p'*-DDT	Methomyl
Simazine	Dibromochloropropane (DBCP)	Methoxychlor (MC)
2,4,5-Trichlorophenoxyacetic acid	Dieldrin	Octachlorostyrene
Trifluralin	α-benzoepin	Oxychlordane
	β-benzoepin	Transnonachlor
Plastics,Epoxies,Polystyrenes		
Bisphenol A	**Pesticides**	
Dibutyl phthalate (DBP)	Benomyl	
Dicyclohexyl phthalate (DBHP)	Vinclozolin	
Diethyl phthalate (DEP)		
p-(1,1,3,3-Tetramethybutyl)phenol (TMBP)		
Diethylhexyl phthalate	**Others**	
Nonylphenol	Benzo(a)pyrene (BAP)	4-Nitrotoluene
Diethylhexyl adipate (DOA)	Benzophenone	Tributyltin chloride
p-Octylphenol (OP)	n-Butylbenzene	Triphenyltin chloride

(Invitrogen) and random hexamers according to the manufacturer's instructions, and PCR was performed using cDNAs as template according to the protocol as previously reported (Zhao et al., 2008) using primers for *CYP3A4* and human *β-actin*. PCR products were separated on 5% polyacrylamide gels and visualized by fluorescence using image scanner. The primers for *CYP3A4* and *β-actin* were as follows: *CYP3A4* sense: 5′-GTGCTGGCTATCACAGATCC-3′, *CYP3A4* antisense: 5′-GACAGAGCTTTGTGGGACTC-3′; *β-actin* sense: 5′-TCGTGCGTGACATTAAGGAG-3′ *β-actin* antisense: 5′-GATGTCCACGTCACACTTCA-3′.

3. Results

3.1. Identification of EDCs enhancing SXR-mediated transactivation

To identify the EDCs which can induce transcription of *CYP3A* genes mediated by SXR, we performed luciferase assay using reporter plasmid ptkCYPDR3×3luc or ptkCYPER6×3luc (DR3 or ER6 sequence as in Table 2) cotransfected with pHSXR into CV-1 cells with treatment of 55 EDCs (Table 1). Either corticosterone, rifampicin or troglitazone was used as a positive control, and thus was found to exert SXR-mediated transactivation of *CYP3A2* and *CYP3A4* (Fig. 1), whereas the induction capacity showing modestly low was closely agreed with the findings of a previous report (Blumberg et al., 1998). Although *p,p'*-DDE had little effect on SXR activity, it was included for comparison with either *p,p'*-DDT or *p,p'*-DDD (Fig. 1).

The chemicals which exerted reproducible inductions of *CYP3A2* (rat *CYP3A*) and *CYP3A4* (human *CYP3A*) in at least 5 independent transfections were shown in Fig. 1. Among these 55 EDCs, 14 chemicals [benzo(a)pyrene, alachlor, nitrofen, nonyphenol, kelthane, methoxychlor, fenvalerate, *p*-Octylphenol, *p,p'*-DDT, *p,p'*-DDD, esfenvalerate, endrin, transnonachlor, TMBP] were found to enhance SXR-mediated transactivation of *CYP3A2* and *CYP3A4* (Fig. 1), and showed to exert dose-dependent transactivation effect on SXR through the promoter region of *CYP3A2* as DR3 (Fig. 2) and *CYP3A4* as ER6 (Fig. 3). Furthermore, these EDCs were revealed to activate SXR-mediated transactivation via βDR4 (sequence as in Table 2) which was identified as the binding site for LXRα found in a promoter region of rat cholesterol 7-α-monooxygenase (*CYP7A1*) gene (Fig. 1), and the 14 chemicals were also shown to have dose-dependent activity (Fig. 4). The PPAR-γ ligand, troglitazone, was also shown to enhance transactivation of SXR in a dose-dependent manner through DR3 of rat *CYP3A2* (Fig. 2B), ER6 of human *CYP3A4* (Fig. 3B), and βDR4 of rat *CYP7A1* (Fig. 4B). Interestingly, *p,p'*-DDE, a metabolite of *p,p'*-DDT, did not activate SXR. The effect of *p,p'*-DDE on SXR action is in contrast to *p,p'*-DDT or *p,p'*-DDD which activated SXR.

3.2. Subcellular localization of SXR with positive EDC

In order to observe the subcellular localization pattern performed by activated SXR in cells, we thus generated a chimeric SXR fused to cyan fluorescence protein (CFP) to construct expressing plasmid pECFP-SXR. The CV-1 cells were transfected with pECFP-SXR and subjected to a confocal microscopic image analysis in the absence or presence of corticosterone or rifampicin (5×10^{-6} M), which activated SXR as shown in Fig. 1 and was used as SXR agonist (Kliewer and Willson, 2002). The results revealed that SXR was diffused in nucleus without the treatment of corticosterone or rifampicin (Fig. 5A); whereas SXR formed intranuclear foci with the treatment of these agonist (Fig. 5B and C). As the relatively strong effect on SXR activation shown in Fig. 1, we selected benzo(a)pyrene as a candidate to examine the subcellular localization pattern of SXR activated by positive EDCs. Similar to corticosterone and rifampicin, SXR also produced fluorescence foci in nucleus after administration of benzo(a)pyrene (Fig. 5D).

Table 2
The sequences for PXRE, SXRE and LXRE.

DR3	PXRE in rat *CYP3A2*	5'-taagcAGTTCAtaaAGTTCAtctac-3'
ER6	SXRE in human *CYP3A4*	5'- tagaataTGAACTcaaaggAGGTCAgtgagtgg-3'
βDR4	LXRE in rat *CYP7A1*	5'-gcggttcccagGGTTTAaataAGTTCAtctaga-3'

The table for PXRE/SXRE/LXRE in the 5′-flanking regions of P450 genes. The uppercase sequences are related to the hexameric consensus binding site for SXR, (A/G)(A/G)(G/T)TCA. The repeated motifs are either direct repeats (DR, arrows pointing in one direction) or everted repeats (ER, arrows pointing away from each other) separated by different numbers of spacer nucleotides (lowercase letter nucleotides). Three copies of DR3 in *CYP3A2*, ER6 in *CYP3A4* or βDR4 in rat *CYP7A1* genes were inserted into the pGL3tk-luc vector.

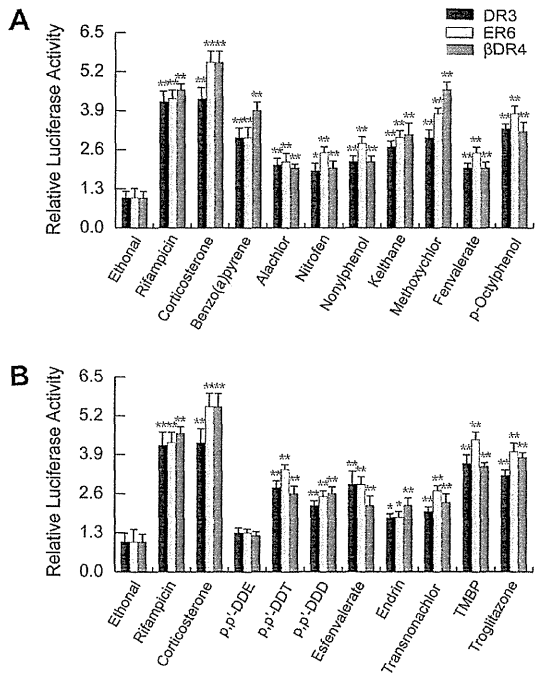

Fig. 1. The effects of the identified EDCs on SXR-mediated transactivation. (A and B) CV-1 cells were transfected with ptkCYPDR3×3luc, ptkCYPER6×3luc or ptkCYPβDR4 together with plasmid expressing SXR. The chemicals (5×10^{-6} M) which showed a positive induction for every DR3-, ER6-type SXRE sequence or βDR4-type LXRE sequence from a representative transfection experiments are shown as increase over the ethanol treated control. Rifampicin, corticosterone and troglitazone were used as positive controls. Although *p,p'*-DDE did not enhance the transactivation of SXR, it was nevertheless included in the figure for comparison purpose with either *p,p'*-DDT or *p,p'*-DDD. Black bars, white bars and weak grey bars represent relative luciferase activities observed in the cells transfected with reporter plasmid ptkCYPDR3×3luc, ptkCYPER6×3luc and ptkCYPβDR4×3luc, respectively. The results represent the mean ± SD of triplicate samples. $^{*}P < 0.05$; $^{**}P < 0.01$ (Student's *t* test) as compared with the ethanol control.

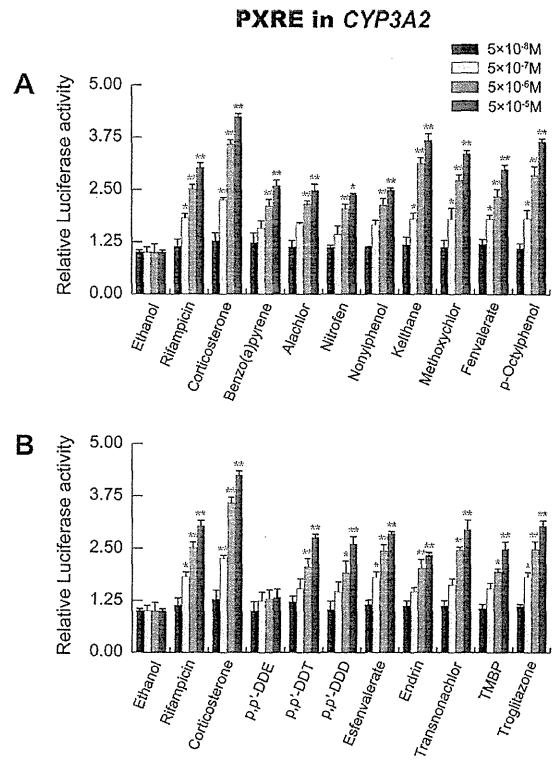

Fig. 2. Dose dependent transactivation of PXRE in *CYP3A2* mediated by SXR bound to chemicals. CV-1 cells were transfected with ptkCYPDR3×3luc together with plasmid expressing SXR. (A) The reporter assay results in the presence of 8 EDCs as well as negative control (ethanol) and positive control (rifampicin, corticosterone); (B) the reporter assay results with the other 7 chemicals and positive control troglitazone. Black bars, white bars, weak grey bars, and dark grey bars represent relative luciferase activities observed in the cells treated with 5×10^{-8}, 5×10^{-7}, 5×10^{-6}, 5×10^{-5} M of chemicals, respectively. The experiments were repeated at least 4 times. The results are presented as the means ± SD. $^{*}P < 0.05$; $^{**}P < 0.01$ (Student's *t* test) as compared with the ethanol control.

3.3. EDCs affected the mRNA expression of CYP3A4 gene

To further verify that *CYP3A4* gene expression was enhanced by the positive EDCs we identified, RT-PCR experiments were performed with compounds as in luciferase assay [rifampicin, corticosterone, benzo(a)pyrene, alachlor, nitrofen, nonyphenol, kelthane, methoxychlor, fenvalerate, *p*-Octylphenol, *p,p'*-DDE, *p,p'*-DDT, *p,p'*-DDD, esfenvalerate, endrin, transnonachlor, TMBP, troglitazone], among them, rifampicin, corticosterone and troglitazone were used as positive controls, and *p,p'*-DDE was used as a comparison with *p,p'*-DDT and *p,p'*-DDD. As shown in Fig. 6, in the absence of EDCs, *CYP3A4* gene weakly expressed in HepG2 cells. With the administration of benzo(a)pyrene, nonylphenol, kelthane, methoxychlor, fenvalerate, *p*-octylphenol, *p,p'*-DDT, *p,p'*-DDD, esfenvalerate and TMBP, the transcript expression of *CYP3A4* was enhanced markedly, and these results were similar to those in the presence of corticosterone, rifampicin and troglitazone. The expression of *CYP3A4* mRNA moderately increased with the treatment of alachlor, nitrofen, endrin and transnonachlor. *p,p'*-DDE barely had effect on the transcript expression of *CYP3A4*.

4. Discussion

In this study, we identified 14 out of 55 EDCs activated SXR-mediated transactivation of human *CYP3A4* gene. These positive EDCs include: (1) pesticides: kelthane; (2) insecticides:methoxychlor, fenvalerate, *p,p'*-DDT, *p,p'*-DDD, esfenvalerate, endrin, transnonachlor; (3) plastics,epoxies,polystyrenes: nonyphenol, *p*-Octylphenol, TMBP; (4) herbicides: alachlor, nitrofen; (5) others: benzo(a)pyrene, which is always found in coal tar. We showed that these positive EDCs also increased endogenous mRNA expression of *CYP3A4* gene in HepG2 cells. In addition to an animal experiment showing that mice carrying human SXR in place of murine PXR exhibited a human type drug metabolism (Xie et al., 2000), our data using a wide variety of synthetic chemicals suspected to be EDCs supported their findings. To date, the mouse model expressing human SXR and CYP3A4 has been established (Cheng et al., 2011), and the in vivo effects of EDCs on *CYP3A4* gene transcription mediated by SXR will be expected to be studied.

Furthermore, our data provide evidence to show that the spectrum of the compounds activating rat *CYP3A2* gene was similar with human *CYP3A4*. These findings are closely agreed with the hypothesis that the species specific drug metabolism mediated by SXR does not depend on SXRE sequence diversity, but instead, mainly depends on the species specific amino acid sequence of the receptor protein (Waxman, 1999). The insecticide, *p,p'*-DDT, or one of its metabolites, *p,p'*-DDD, was found to be an activator of both *CYP3A2* and *CYP3A4*, while another metabolite, *p,p'*-DDE was not. *p,p'*-DDE has been suspected to be an end-metabolite of *p,p'*-DDT, which probably raises the risk of breast cancer (Tarone